Linden Laboratories, Inc.

State College, Pennsylvania 16801

Technical Report No. 1

STRENGTHENING OXIDES BY REDUCTION OF CRYSTAL ANISOTROPY

August, 1967

Prepared by:

Henry P. Kirchner

Robert M. Gruver

Prepared under Contract No. N00014-66-C0190 for the Office of Naval Research, Department of the Navy.

Linden Laboratories, Inc.

State College, Pennsylvania 16801

Technical Report No. 1

STRENGTHENING OXIDES BY REDUCTION OF CRYSTAL ANISOTROPY

August, 1967

Prepared by: Henry P. Kirchner

Henry P. Kirchner

Robert M. Gruver

Robert M. Gruver

Prepared under Contract No. N00014-66-C0190 for the Office of Naval Research, Department of the Navy, Requisition Number NR 032-490.

FOREWORD

This report describes research performed on a program sponsored by the Office of Naval Research, Department of the Navy under Contract N00014-66-C0190. The research was performed under the general technical direction of Dr. Arthur M. Diness of the Office of Naval Research.

The authors are pleased to acknowledge the contributions of their associates at Linden Laboratories including especially Mrs. Violetta Adams, Mr. Ralph E. Walker, Mr. Norman Bierly and Mrs. Helen Cuff. The authors are indebted to Dr. W.R. Buessem for helpful discussions and to Mr. Charles Bulgey of Cornell Aeronautical Laboratory for assistance in measuring the thermal expansion of BeO.

BLANK PAGE

ABSTRACT

An investigation of the effect of crystal anisotropy on the strength of oxides is described. Solid solutions of various materials in rutile (TiO_2) and zincite (ZnO) were prepared and the thermal expansion properties were measured in an attempt to find compositions with reduced anisotropy.

Bodies composed of 72% Al_2O_3-28% Cr_2O_3 were prepared by reactive hot pressing. Preliminary evidence of a strengthening effect compared with pure Al_2O_3 is presented.

LIST OF FIGURES

LIST OF TABLES

TABLE OF CONTENTS

BLANK PAGE

I. INTRODUCTION

Three possibilities provide the principal motivations for investigations of the thermal expansion of solid solutions of ceramic materials. One of these is the use of low-expansion solid solutions for chemical strengthening of polycrystalline ceramic bodies in a manner analogous to the chemical strengthening of glasses. If low expansion surface layers are formed on bodies at high temperatures, the bodies tend to contract more than the surface layers during subsequent cooling, placing the surface layers in compression. The feasibility of chemical strengthening of alumina, titania and spinel ceramics by low-expansion solid solution surface layers has been established.[1-3]

Another possibility is the use of solid solutions with reduced thermal expansion anisotropy and/or elastic anisotropy to obtain smaller localized stresses between grains in polycrystalline bodies and thereby obtain improved properties. When a single phase body consisting of anisotropic crystals is sintered at high temperatures, little stress is present between the individual crystals. However, during cooling the individual crystals tend to contract more in the high expansion directions than in the low expansion directions giving rise to localized stresses in the grain boundaries and in the crystals. In addition, localized stresses arise as a result of elastic anisotropy. These stresses result from the way in which the applied loads, large scale residual stresses, and localized stresses are transmitted through elastically anisotropic media.

The importance of these localized stresses has been discussed by Buessem et al,[4] Clarke,[5] Buessem and Lange[6] and others. An analytical method for estimating the localized stresses resulting from thermal expansion anisotropy was presented.[6] Reduction of the thermal expansion anisotropy of rutile (TiO_2) and cassiterite (SnO_2) by addition of vanadium in solution was reported by Merz, Brown, and Kirchner.[7] Similar results were achieved for corundum (Al_2O_3) by addition of chromium in solution.[8]

A third possibility is that the study of these solid solutions can lead to a better understanding of the roles of various ionic species in the dynamics of the lattice, thus leading to a more complete understanding of the equations of state of oxide materials. Investigations of these last two possibilities are the objective of this research.

Some oxide solid solution systems that were investigated previously include a large number of compositions involving TiO_2 as one component, and compositions in the systems SnO_2-VO_2 and Al_2O_3-Cr_2O_3 all reported by Merz, Brown and Kirchner,[7] Al_2O_3-Cr_2O_3 reported by Stradley, Shevlin and Everhart,[9] Zn_2SiO_4-Mg_2SiO_4 and Zn_2GeO_4-Mg_2GeO_4 reported by Wen, Brown and Hummel,[10] and for a variety of solid solutions in zinc phosphates and vanadates reported by Brown and Hummel.[11]

In this report, the results of thermal expansion measurements of end members and solid solutions of materials having tetragonal and hexagonal structures are presented. These results are discussed in terms of the characteristics of the added ions.

In addition, polycrystalline ceramic bodies were prepared from compositions with reduced expansion anisotropy in the Al_2O_3-Cr_2O_3 and TiO_2-VO_2 systems. The flexural strengths of these bodies in the Al_2O_3-Cr_2O_3 system are reported and compared with the flexural strengths of pure alumina bodies of comparable grain size and porosity. These preliminary results indicate that strengthening was achieved.

II. THERMAL EXPANSION ANISOTROPY OF RUTILE STRUCTURE OXIDES AND SOLID SOLUTIONS

(A). Selection of Materials for Investigation

In earlier research the thermal expansion anisotropy of rutile structure materials (stishovite, SiO_2[12]; GeO_2[13]; rutile, TiO_2[7]; and cassiterite, SnO_2[7]) was investigated. In stishovite and tetragonal GeO_2, the thermal expansion in the "a" axis direction is greater than in the "c" axis direction whereas in rutile and cassiterite it is lower. In the cases studied previously it seemed that crystals with smaller cations tended to have higher expansion in the "a" axis direction than in the "c" axis direction and conversely for those with larger cations.

Knowledge of the factors governing the effect of various solid solution atoms on the expansion anisotropy will be helpful in finding compositions with reduced anisotropy. As an aid in determining these factors, more data on pure oxides with the rutile structure are needed, so it was decided to attempt to measure the expansion anisotropy of tetragonal VO_2. This material is of special interest because addition of vanadium to rutile and cassiterite caused substantial modification of the expansion anisotropy of those phases. In studying this material, it may be possible to determine whether the change in anisotropy observed in these phases results from the properties of the vanadium or is mainly a result of changes in the lattice constants or defect structure when the vanadium is added.

In addition to the pure oxides, solid solutions of GeO_2, Sc_2O_3, $Sc_2O_3 + V_2O_5$, Ga_2O_3 and $Ga_2O_3 + V_2O_5$ in TiO_2 were investigated. The solid solutions of GeO_2 in TiO_2 were selected for investigation because extensive solid solution is indicated in the phase diagram and earlier measurements[8] had indicated reduction of the expansion anisotropy when small percentages of germanium were present in rutile. Investigation of the compositions containing scandium and vanadium, and gallium and vanadium was done in order to determine whether or not the effectiveness of vanadium in reducing the expansion anisotropy of rutile was primarily a result of the presence of a smaller cation or perhaps a result of other effects such as changing the valence state of some of the titanium atoms, or changes in the lattice constants of the material.

(B). Sample Preparation

VO_2 was purchased from City Chemical Company. In the "as received" condition the material was poorly crystallized so that no diffraction peaks were observed in the back-reflection region. Therefore, the material was reheated under various conditions (atmosphere, time, temperature) in an effort to improve the diffraction pattern. After several attempts, treatments at 1000°C for six hours in a helium atmosphere gave several diffraction peaks in the back-reflection region. A small percentage of material other than VO_2 was present. The thermal expansion measurement was made in a flowing helium atmosphere.

The rutile solid solutions were prepared by heating the mixed oxides. In some cases the samples were quenched in an attempt to improve the sharpness of the peaks in the back-reflection region of the X-ray diffraction patterns.

(C). Procedures for X-ray Measurements

A General Electric XRD-5 diffractometer with a copper tube (λ=1.54050 Å for K_α) and a Hem-Prep high temperature X-ray diffraction furnace were used. Lines in the back-reflection region were used to attain precision and accuracy in the determination of the lattice constants. In some cases, considerable difficulty with misshapen peaks was encountered. The peak positions were taken as the midpoint at an arbitrary distance from the top of the peak or as the midpoint at one-half peak height, depending upon the shape of the peak and the separation of the K_{α_1} and K_{α_2} peaks.

(D). Results and Discussion

Vanadium dioxide (VO_2). The best of the thermal expansion results for VO_2 are presented in Table I and Figure 1. These results are considered to be tentative because of problems associated with indexing the diffraction pattern, poor diffraction peak shape and sample stoichiometry. Nevertheless, it is hoped that these data will not be too different from the results of better measurements.

Because of the monoclinic to tetragonal phase transformation

TABLE I

Thermal Expansion of Tetragonal VO_2

1000°C for 6 hours in helium

Pattern No. 67

Temp. °C	Angle 213	Angle 422	d_{213}	d_{422}	a_o	Δa	% Exp	c_o	Δc	% Exp
100	126.772	136.790	.86153	.82846	4.5514	-	-	2.8527	-	-
200	126.415	136.413	.86288	.82953	4.5559	.0045	.10	2.8575	.0048	.17
300	125.882	136.031	.86493	.83065	4.5593	.0079	.17	2.8653	.0126	.44
400	125.478	135.685*	.86649	.83166	4.5630	.0156	.25	2.8712	.0185	.65

* very poor peak

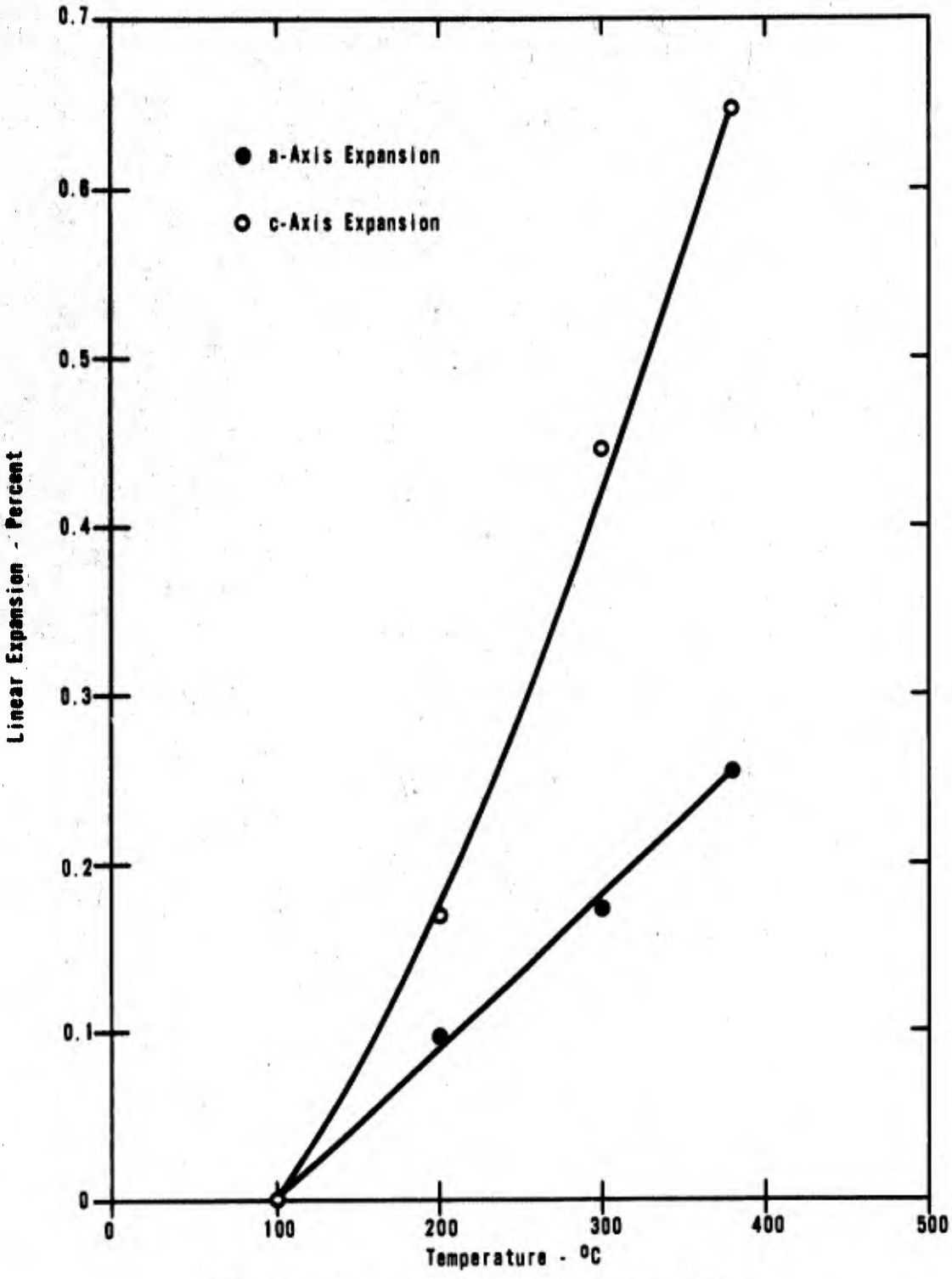

Figure 1 Thermal Expansion of Tetragonal VO_2

in VO_2 at about 66°C, the measurements were started at 100°C and continued at 100°C intervals up to 500°C. At 500°C the pattern was so poor that results were not obtained. The "c" axis expansion is much greater than the "a" axis expansion.

In Table II these new results are compared with previous results obtained for other rutile structure oxides listed in order of increasing cation radius. It is evident from this comparison that factors other than the cation radius are important in determining the expansion anisotropy.

The thermal expansion of crystals depends upon two principal factors; the tendency of the ions to vibrate and exert pressure on the lattice (the so-called thermal pressure), and the resistance of the lattice to expansion which depends in turn on the elastic constants. The tendency of the ions to vibrate varies with temperature. The tendency of the vibrations to exert pressure on the lattice is related to structural characteristics including the symmetry of the structure and the presence of open space in the lattice into which the ions can vibrate with less pressure exerted on the lattice. In general, one expects to observe high expansion coefficients in phases with highly symmetrical, densely packed structures having low values of the elastic stiffness constants. Phases with low symmetry, open structures and high elastic constants tend to have low expansion coefficients.

The transition metal oxide phases with the rutile structure are more densely packed than the phases with group IV-A cations. This increase in packing density is illustrated in Figure 2 in

TABLE II

Thermal Expansion Data for Oxides with the Rutile Structure
(Room Temperature to 400°C)

Material	Lattice Parameters Å		Thermal Expansion Coefficients ($°C^{-1}$) $X10^7$		Anisotropy Ratio	Cation Radius Å
	a_o	c_o	α_a	α_a	α_a/α_c	
SiO_2 [12] (stishovite)	4.1792	2.6648	66	41	1.6	0.42
GeO_2 [13]	4.398	2.862	80	37	2.2	0.53
VO_2*	4.551	2.853	85	214	0.40	0.63
TiO_2 [7] (rutile)	4.5937	2.9593	80	101	0.80	0.68
SnO_2 [7] (cassiterite)	4.738	3.188	43	56	0.77	0.71

* preliminary data

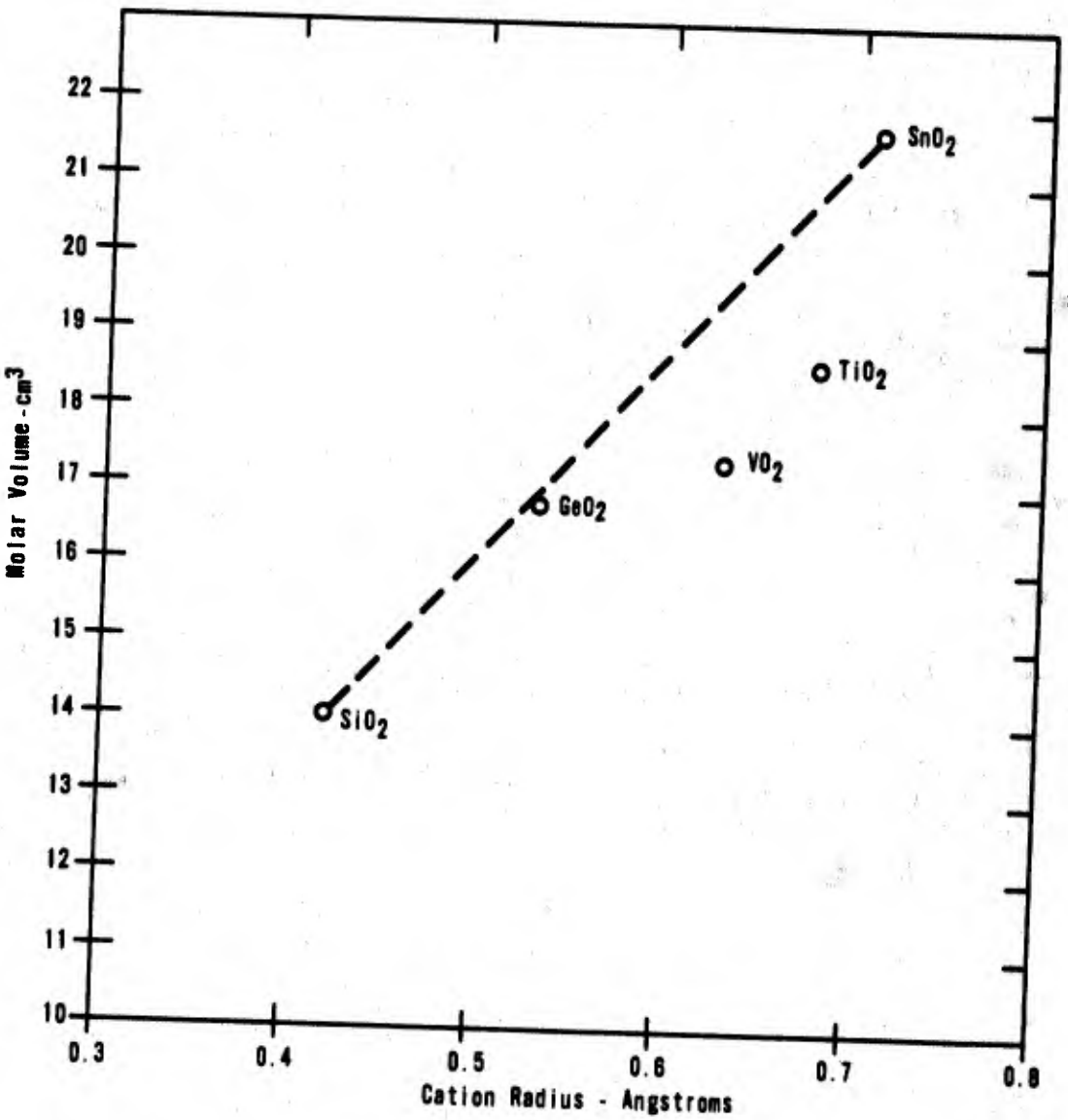

Figure 2 Molar Volume Vs. Cation Radius for Rutile Structure Oxides

which molar volumes of the oxides of titanium and vanadium fall below the values expected for cations of their particular sizes based upon the lattice constants observed for the phases with group IV-A cations. Based upon the factors discussed in the previous paragraph, the volume expansion coefficients of TiO_2 and VO_2 are expected to be relatively high. The volume expansion coefficients presented in Table III show that these higher volume expansion coefficients were observed.

TABLE III

Volume Thermal Expansion Coefficients
of Rutile Structure Oxides
(Rm T - 400°C)

Material	Volume Expansion Coefficient
SiO_2 (stishovite)	173×10^{-7} °C^{-1}
GeO_2	197×10^{-7}
VO_2*	384×10^{-7}
TiO_2 (rutile)	261×10^{-7}
SnO_2 (cassiterite)	142×10^{-7}

*preliminary data

Extending this same type of argument to the comparison of differences between the observed lattice constants and the lattice constants expected based upon changes in cation radii, with the thermal expansion coefficients in the different crystallographic directions, it is evident that the lattice

constants that are larger than expected are associated with lower values of expansion coefficient in the same direction and vice versa. Using the lattice constants of the composition 0.90 TiO_2-0.10 VO_2 as a basis for comparison because it has a small expansion anisotropy, the above-mentioned differences are presented in Table IV. As expected, the lower expansion materials have the more positive differences indicating that the lattice constants are larger than expected. In addition, the larger positive values for SiO_2 and GeO_2 are associated with c_o which is the low expansion direction in each of these phases. The larger negative value, meaning that the lattice constant is smaller than expected is associated with the c_o for TiO_2 and VO_2 which is the high expansion direction. The magnitudes of the lattice constants of SnO_2 yield differences that are inconsistent with this line of reasoning for reasons that are not understood at present.

This observation of a relationship involving the difference between the actual lattice constants and those predicted, and the thermal expansion anisotropy, may be of great importance in further work on this program. It is hoped that by looking for large differences between measured lattice constants and those expected based upon changes in cation radii, it will be possible to find solid solution compositions in which there are substantial changes in thermal expansion anisotropy.

TABLE IV

Differences Between Observed Lattice Constants and Those Expected from Variations in Cation Radii

(Based upon lattice constants of 0.90 TiO_2 + 0.10 VO_2 $a_o = 4.5853$, $c_o = 2.9581$)

Material	Lattice Parameters a_o	Lattice Parameters c_o	Observed Change In Lattice Parameters a_o	Observed Change In Lattice Parameters c_o	Expected Change* x	Differences $a_o - x$	Differences $c_o - x$
SiO_2(stishovite)	4.1792	2.6648	-0.4061	-0.2933	-0.50	+0.094	+0.207
GeO_2	4.398	2.862	-0.187	-0.096	-0.28	+0.093	+0.184
VO_2	4.551	2.853	-0.034	-0.105	-0.09	+0.056	-0.015
TiO_2(rutile)	4.5937	2.9593	+0.0069	-0.0003	+0.02	-0.013	-0.020
SnO_2(cassiterite)	4.738	3.188	+0.1527	+0.230	+0.08	+0.073	+0.150

* Average cation radius for 0.90 TiO_2 + 0.10 VO_2 is 90°.68 + 10°.63 = 0.675. There are two cations per unit cell. Therefore the expected change is $2(r_c - 0.675)$ where r_c is the cation radius.

TiO_2-GeO_2 solid solutions. The solid solutions were formed by heating the mixed oxides. In general, the back-reflection peaks were broad and not useable. Fair results were obtained by heating to 1400 or 1500°C followed by quenching into water. The samples used for the X-ray measurements were prepared by this method.

Thermal expansion curves for solid solutions of GeO_2 in TiO_2 having three different nominal compositions are given in Figure 3. The actual compositions were estimated from the lattice constants assuming that Vegard's Law is applicable between the end members. The degree to which Vegard's Law is actually applicable is not known. These estimates are given in Table V. They indicate that only part of the available GeO_2 entered the solution and all of the expansion curves represent solid solution compositions in the range 7-9% GeO_2. With this added information, it is apparent that the presence of GeO_2 in solution in TiO_2 leads to reduction of the expansion coefficients in the "a" and "c" directions and a small reduction in thermal expansion anisotropy.

Since the compositions, estimated from the changes in lattice constants, agree when determined by both a_o and c_o, the proportions of the unit cell seem to change in the way predicted from the unit cell dimensions of the end members. In this case, then, we expect to observe little difference between the actual lattice constants and the expected lattice constants (if the composition were known independently) so, based on the earlier discussed approach a marked change in expansion anisotropy

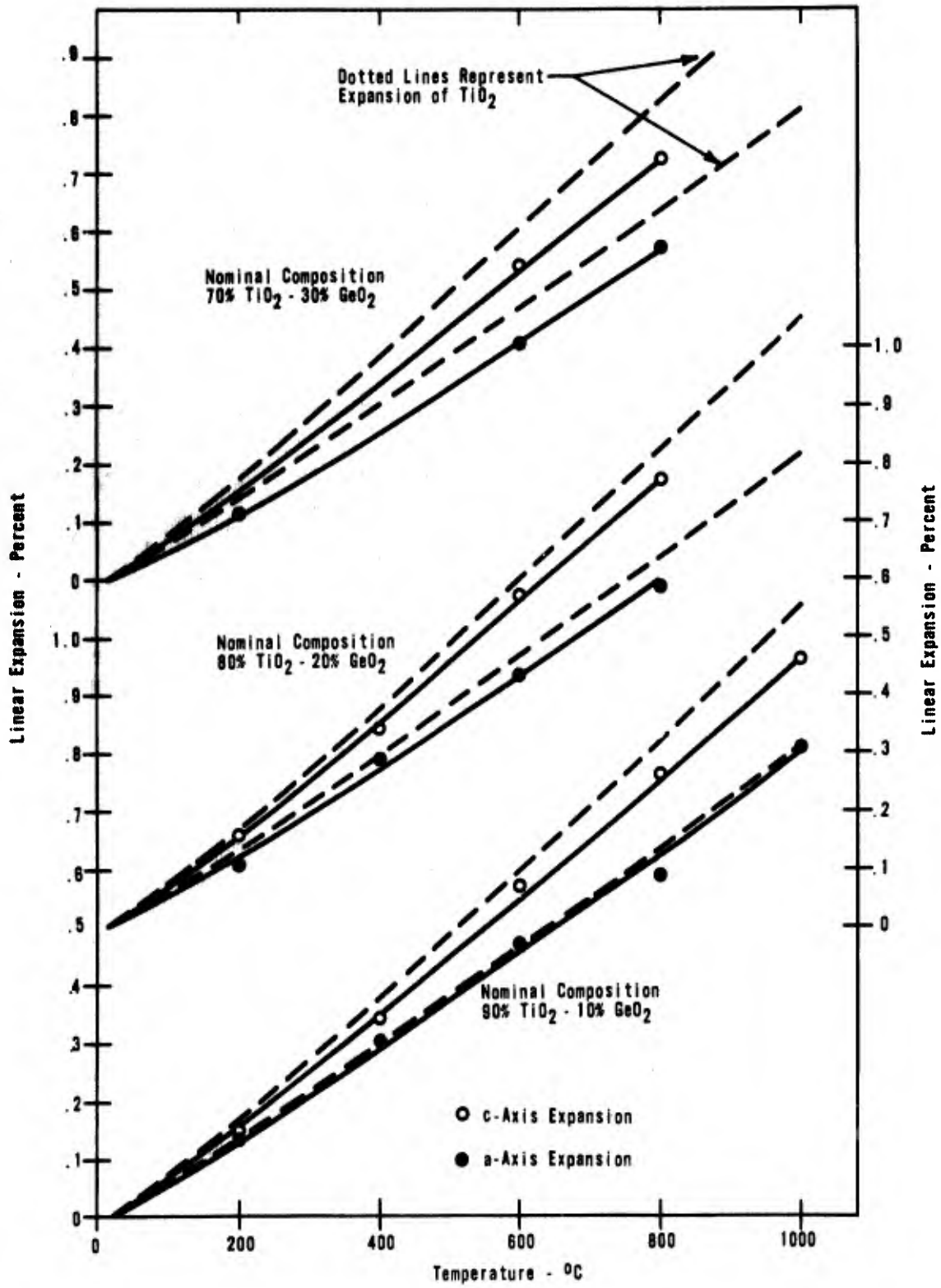

Figure 3 Thermal Expansion of TiO_2-GeO_2 Solid Solutions

TABLE V

Estimated Compositions of TiO_2-GeO_2 Solid Solutions

Nominal Compositions	Lattice Constants a_o	c_o	Estimated Compositions Based on a_o	Based on c_o	Ave.
100% TiO_2	4.5922 Å	2.9578 Å	-	-	-
90% TiO_2 - 10% GeO_2 (Pattern No. 20)	4.5788	2.9509	7% GeO_2	7% GeO_2	7% GeO_2
80% TiO_2 - 20% GeO_2 (Pattern No. 31)	4.5757	2.9489	8.5% GeO_2	9% GeO_2	9% GeO_2
70% TiO_2 - 30% GeO_2 (Pattern No. 32)	4.5744	2.9493	9% GeO_2	9% GeO_2	9% GeO_2
100% GeO_2	4.398*	2.862*	-	-	-

*Data from J.F. Sarver, "Thermal Expansion of Rutile-Type GeO_2" J. Am. Ceram. Soc. 46(4) 195-196 (April, 1963).

would not be expected and was not observed.

The volume expansion of 91% TiO_2 - 9% GeO_2 of about 224×10^{-7}/°C (25-400°C) is much lower than one would expect based upon a linear extrapolation between the end members. The fact that neither the expansion anisotropy nor the volume expansion obeys a linear extrapolation between the end members is additional evidence that the expansion anisotropy depends on the changes in the individual lattice constants.

TiO_2-Sc_2O_3 solid solutions. The composition 90% TiO_2-10% $1/2Sc_2O_3$ was prepared by heating at 1400°C for two hours. The lattice constants of the resulting rutile were $a_o = 4.5931$ and $c_o = 2.9596$, not significantly different from those of pure TiO_2, indicating that little, if any, scandium went into solution in the TiO_2. The thermal expansion curve, given in Figure 4, indicates little or no change in expansion from that of rutile.

TiO_2-Sc_2O_3-VO_2 solid solutions. The composition 80% TiO_2 + 10% $1/2Sc_2O_3$ + 10% VO_2 was prepared by firing the oxide mixture at 1150°C for one hour. The lower firing temperature was used because of the volatility of vanadium oxide. X-ray analysis indicated the presence of some unreacted vanadium oxide but no unreacted Sc_2O_3. In this case the normally 4-valent vanadium can change its valence to +5, allowing the 3-valent scandium to be dissolved in the lattice. The effects of the smaller vanadium ion (0.63Å) and the larger scandium

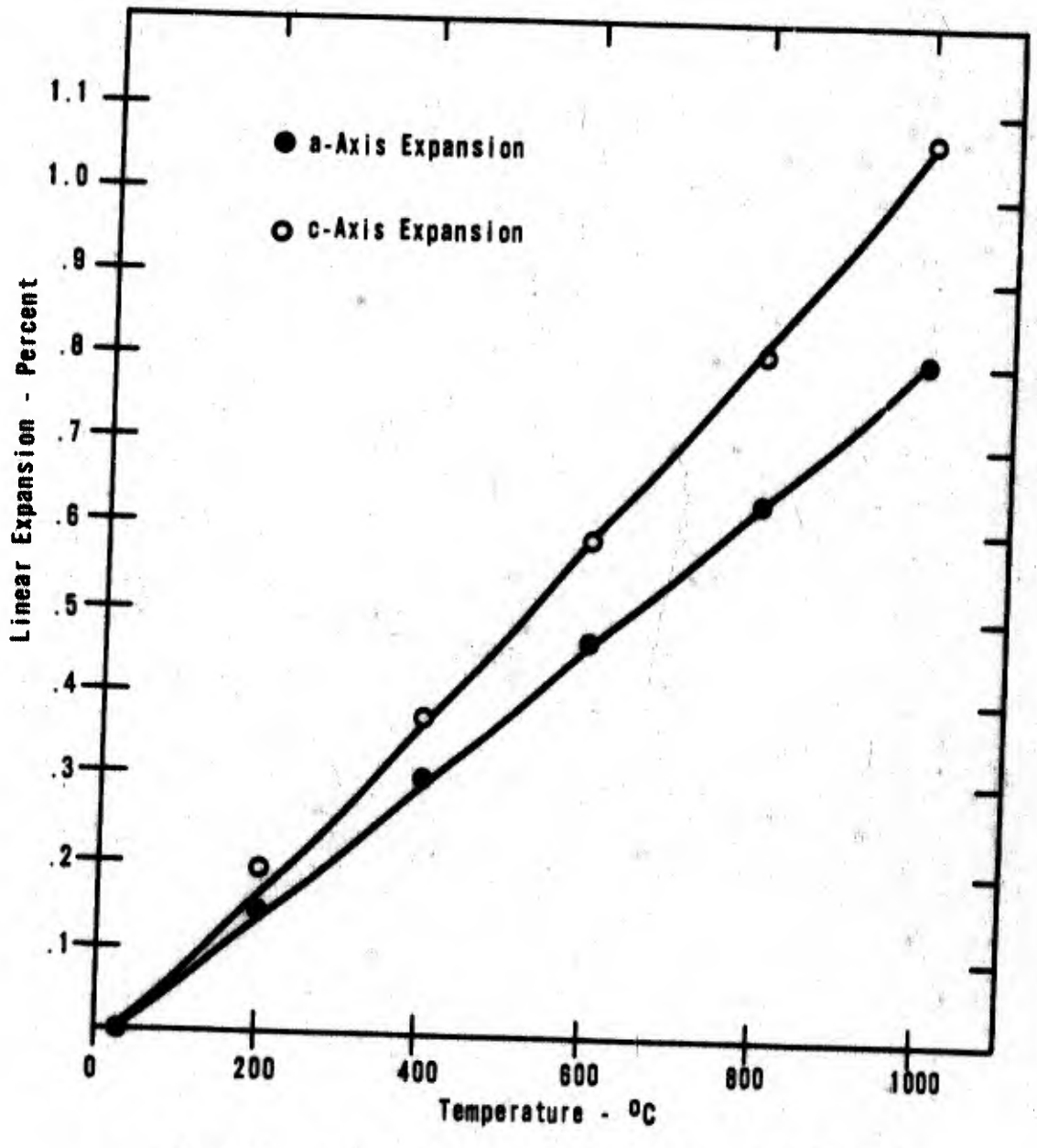

Figure 4 Thermal Expansion of 90% TiO_2 - 10% $1/2Sc_2O_3$

ion (0.81Å) counteract each other and little change in the lattice constants is observed. The thermal expansion data are given in Table VI and in Figure 5 these data are compared with data for pure TiO_2 and 90% TiO_2 + 10% VO_2. The thermal expansion coefficients in the "a" axis and "c" axis directions, and the thermal expansion anisotropy are substantially reduced, compared with those of pure TiO_2. However, the expansion anisotropy was not drastically lowered as it was in the case of 90% TiO_2 + 10% VO_2.

TiO_2-Ga_2O_3 solid solutions. The composition 90% TiO_2 + 10% 1/2 Ga_2O_3 was prepared by firing the oxide mixture at 1150°C for one hour. X-ray diffraction analysis showed a small decrease in the lattice constants indicating some solid solution formation and some unreacted Ga_2O_3. The radius of Ga^{3+} is 0.62Å.

The thermal expansion data are given in Table VII and, in Figure 6, these data are compared with data for pure TiO_2. The thermal expansion in the "a" axis direction is reduced by addition of Ga_2O_3. The thermal expansion anisotropy is also somewhat reduced.

TiO_2-Ga_2O_3-VO_2 solid solutions. The compositions 80% TiO_2 + 10% 1/2Ga_2O_3 + 10% VO_2 and 60% TiO_2 + 20% 1/2Ga_2O_3 + 20% VO_2 were prepared by firing the oxide mixtures at 1150°C for one hour. The X-ray patterns indicate some unreacted V_2O_5 but little or no unreacted Ga_2O_3. The lattice parameters

TABLE VI

Thermal Expansion Data

80% TiO_2 + 10% V_2O_5 + 10% $1/2Sc_2O_3$

Fired at 1150°C for 1 hour

Pattern No. 41

Temp. °C	Angle 213	Angle 521	d_{213}	d_{521}	a_o	Δa	% Exp	c_o	Δc	% Exp
Rm. T	120.024	140.039	.88930	.81958	4.5931	-	-	2.9596	-	-
200	119.796	139.698	.89033	.82048	4.5982	.0051	.11	2.9631	.0035	.12
400	119.372	139.186	.89225	.82183	4.6055	.0124	.27	2.9699	.0103	.35
600	118.996	138.680	.89396	.82320	4.6131	.0200	.43	2.9757	.0161	.54
800	118.636	138.162	.89562	.82461	4.6209	.0278	.60	2.9814	.0218	.73
1000	118.252	137.000	.89742	.82597	4.6282	.0351	.76	2.9876	.0280	.94

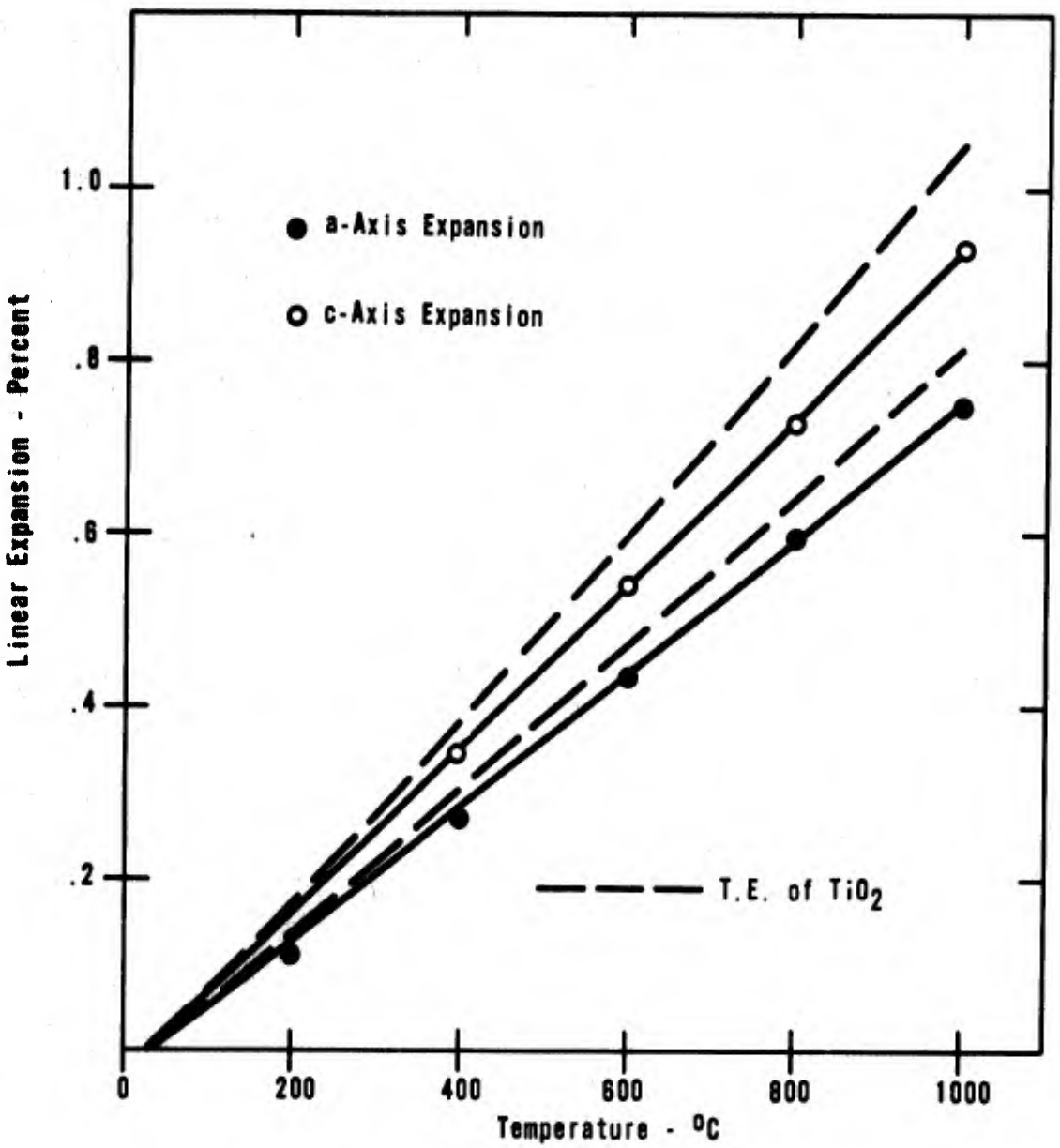

Figure 5 Thermal Expansion of 80% TiO_2 + 10% $1/2Sc_2O_3$ + 10% VO_2 (Pattern No. 41, Using 213,521)

TABLE VII

Thermal Expansion Data
90% TiO_2 + 10% $1/2Ga_2O_3$
Fired at 1150°C for 1 hour
Pattern No. 60
(Not completely reacted)

Temp. °C	Angle 213	Angle 521	d_{213}	d_{521}	a_o	Δa	% Exp	c_o	Δc	% Exp
Rm. T	120.145	140.148	.88876	.81930	4.5917	-	-	2.9576	-	-
200	119.882	139.648	.88993	.82061	4.6009	.0092	.20	2.9613	.0037	.12
400	119.485	139.271	.89173	.82161	4.6044	.0127	.28	2.9679	.0103	.35
600	119.065	138.747	.89365	.82301	4.6121	.0204	.44	2.9746	.0170	.57
800	118.637	138.184	.89562	.82455	4.6216	.0299	.65	2.9817	.0241	.81
1000	118.205	137.610	.89764	.82613	4.6292	.0375	.81	2.9884	.0308	1.03

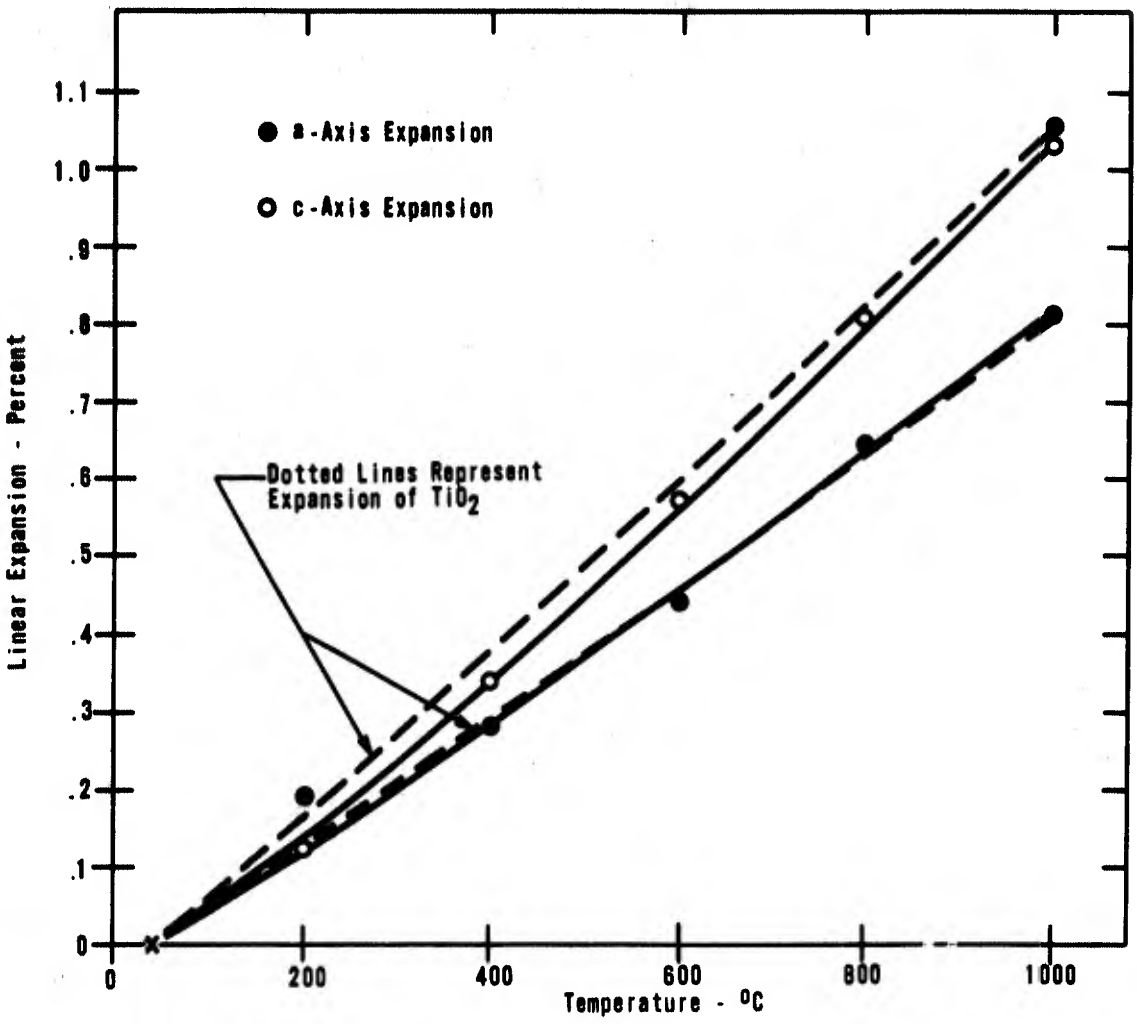

Figure 6 Thermal Expansion of 90% TiO_2 + 10% $1/2Ga_2O_3$

decreased as expected as a result of adding two different ions both smaller than Ti^{4+}.

The thermal expansion data are presented in Tables VIII and IX and Figure 7. The thermal expansions in the "a" and "c" axis directions are reduced compared with TiO_2. The thermal expansion anisotropy is reduced especially for 60% TiO_2 + 20% $1/2Ga_2O_3$ + 20% VO_2.

These results for compositions in the TiO_2-Ga_2O_3-VO_2 system are very similar to the results obtained for the composition in the TiO_2-Sc_2O_3-VO_2 system which had larger lattice constants. This comparison provides additional evidence that the reduction in expansion anisotropy does not result mainly because of adding small ions as was previously suggested but depends mainly on other factors.

TABLE VIII

Thermal Expansion Data

80% TiO_2 + 10% $1/2V_2O_5$ + 10% $1/2Ga_2O_3$

Tetragonal

Fired at 1150°C for 1 hour

Pattern No. 56

Temp. °C	Angle 213	Angle 521	d_{213}	d_{521}	a_o	Δa	% Exp	c_o	Δc	% Exp
Rm. T	120.343	140.461	.88788	.81849	4.5872	-	-	2.9547	-	-
200	120.080	140.088	.88907	.81945	4.5925	.0053	.12	2.9588	.0041	.14
400	119.691	139.557	.89080	.82084	4.6002	.0130	.28	2.9648	.0101	.34
600	119.325	139.044	.89246	.82221	4.6078	.0206	.45	2.9704	.0157	.53
800	118.958	138.517	.89414	.82362	4.6156	.0284	.62	2.9761	.0214	.72
1000	118.488	137.920	.89632	.82527	4.6246	.0374	.81	2.9837	.0290	.97

TABLE IX

Thermal Expansion Data
60% TiO_2 + 20% $1/2Ga_2O_3$ + 20% VO_2
tetragonal
Fired at 1150°C for 1 hour
Refired at 1150°C for 1 hour and quenched
Pattern No. 69

Temp. °C	Angle 521	Angle 213	d_{521}	d_{213}	a_o	Δa	% Exp	c_o	Δc	% Exp
Rm. T	140.798	120.426	.81763	.88751	4.5821	-	-	2.9539	-	-
200	140.455	120.248	.81850	.88830	4.5870	.0050	.11	2.9564	.0025	.08
400	139.917	119.879	.81990	.88995	4.5948	.0127	.28	2.9607	.0067	.23
600	139.321	119.536	.82147	.89150	4.6037	.0216	.47	2.9671	.0132	.44
800	138.791	119.142	.82289	.89330	4.6115	.0295	.64	2.9733	.0194	.65
1000	138.198	118.700	.82450	.89533	4.6204	.0383	.83	2.9803	.0263	.88

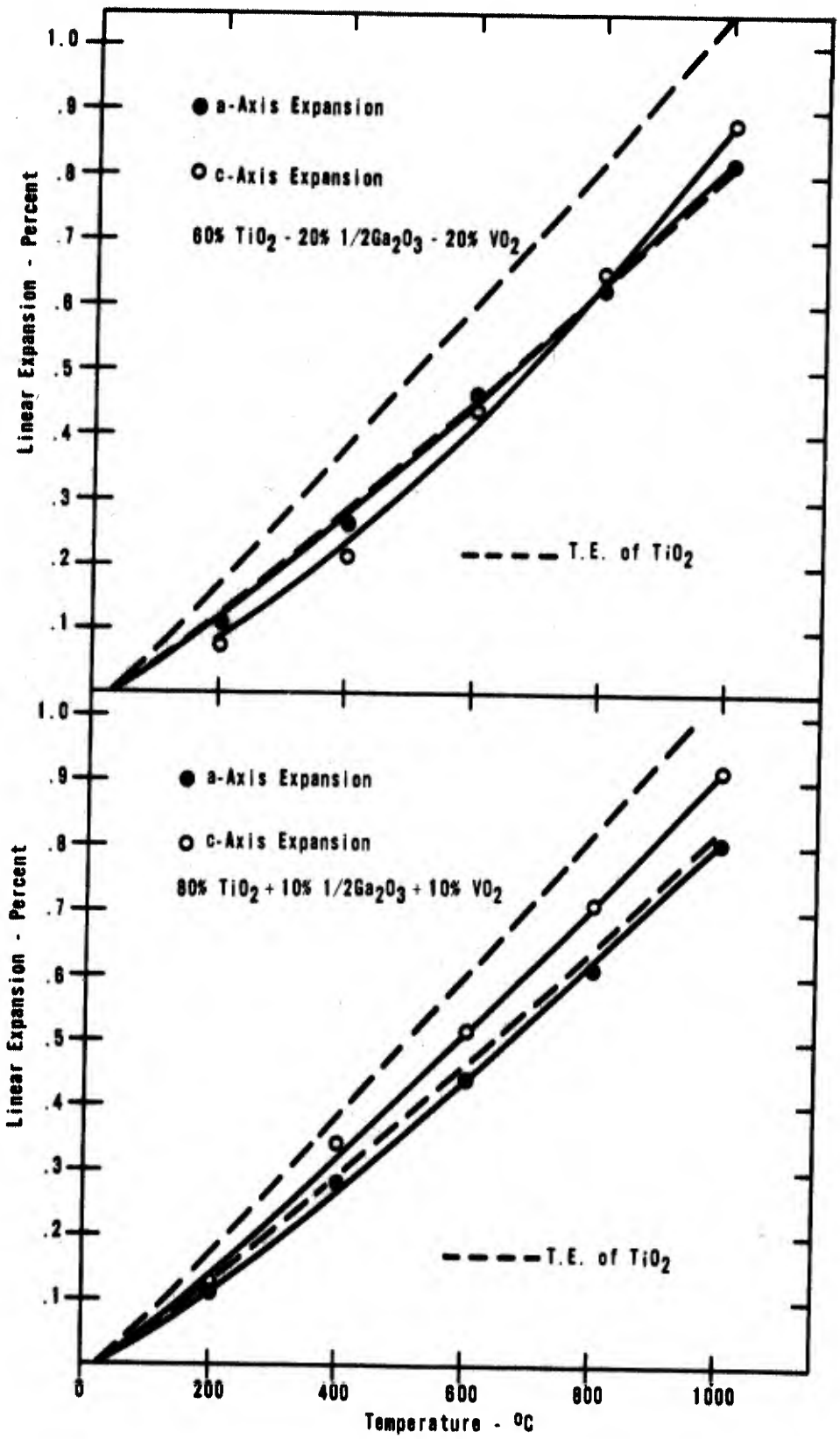

Figure 7 Thermal Expansion of Solid Solutions in the TiO_2 - Ga_2O_3 - VO_2 System

III. THERMAL EXPANSION ANISOTROPY OF ZnO AND ZnO SOLID SOLUTIONS

(A). Selection of Materials for Investigation

One objective of the present program is to attempt to determine relationships between thermal expansion anisotropy and elastic anisotropy. Substantial effort has been devoted by others to investigation of the anisotropic properties of hexagonal phases (graphite, zinc and cadmium metal, etc.). Using thermal expansion data, Debye temperatures and volume compressibilities Riley[14] estimated certain elastic constants for graphite. Because of the availability of the results of related work on hexagonal crystals, it was decided to investigate modification of the thermal expansion anisotropy of hexagonal oxides. Because of its rather large expansion anisotropy, zinc oxide was chosen as the material for this part of the investigation.

A search of available phase equilibrium diagrams[15] showed that few of the systems involving zinc oxide have been investigated and of those that have been studied few show any solid solution formation. In addition, it is reasonable to expect some limitation of solid solution formation because of the tendency of Zn^{2+} toward tetrahedral coordination. Nevertheless, many of the oxide systems having cations with radii near that of Zn^{2+} (0.74Å) have not been investigated and solid solution formation in some of these systems is a reasonable expectation. Based upon similarities in ionic radii or structures

several oxides were reacted with ZnO in an attempt to form solid solutions with modified expansion anisotropy. In addition, solid solutions of vanadium in ZnO were investigated because of the substantial effect that vanadium has on the expansion anisotropy of rutile (TiO_2) and cassiterite (SnO_2). The results of these experiments are discussed in the following paragraphs.

(B). Sample Preparation

Fisher certified ZnO was used for these measurements. The solid solutions were prepared by heating the mixed oxides in air as described more completely in the following sections.

(C). Results and Discussion

Zinc oxide. The thermal expansion data for zinc oxide are presented in Table X and Figure 8. The observed room temperature lattice constants were $a_o = 3.2484$ and $c_o = 5.2040$, comparing favorably with those of Swanson and Fuyat[16] which were $a_o = 3.249$ and $c_o = 3.205$. The thermal expansion in the "a" axis direction was somewhat higher than that observed by Beals and Cook[17] while that in the "c" axis direction was somewhat lower than was observed by the same authors. In spite of these differences, the agreement is reasonable considering the usual errors in measurement and the rather unusual shape of the curves in the cited reference. Substantial thermal expansion anisotropy was observed.

TABLE X

Thermal Expansion Data
ZnO
Pattern No. 11A

Temp. °C	Angle 205	Angle 220	d_{205}	d_{220}	a_o	Δa	% Exp	c_o	Δc	% Exp
Rm. T	134.034	143.054	.83666	.81209	3.2484	-	-	5.2040	-	-
200	133.818	142.684	.83733	.81298	3.2519	.0036	.11	5.2073	.0033	.06
400	133.514	142.184	.83829	.81419	3.2568	.0084	.26	5.2123	.0083	.16
600	133.190	141.616	.83931	.81558	3.2623	.0140	.43	5.2173	.0133	.26
800	132.868	141.036	.84033	.81703	3.2681	.0198	.61	5.2220	.0180	.35
1000	132.536	140.400	.84140	.81864	3.2746	.0262	.81	5.2267	.0217	.42

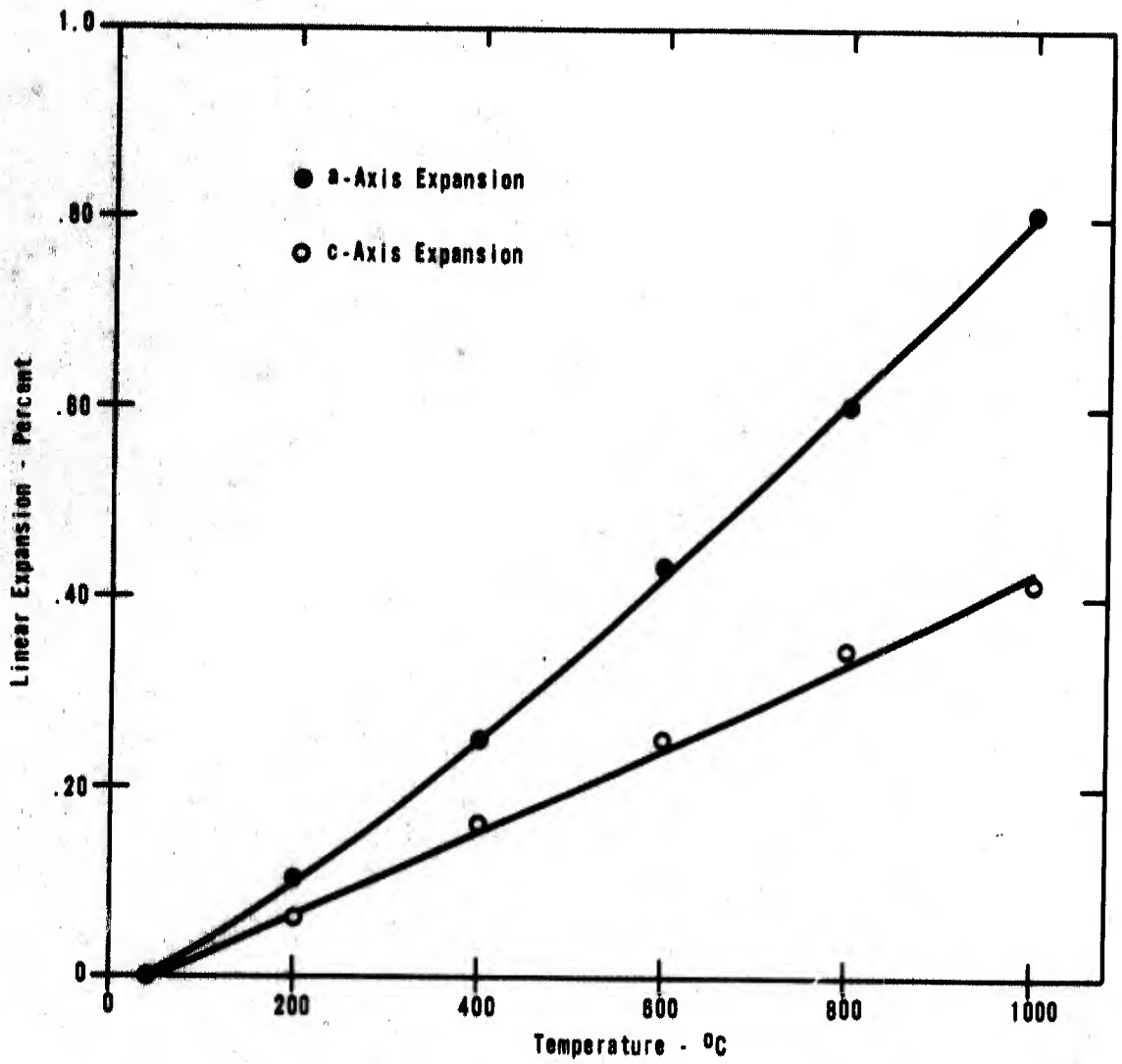

Figure 8 Thermal Expansion of Zinc Oxide
(Pattern No. 11A, Miller Indices 205,220)

ZnO-SnO solid solutions. Mixtures of ZnO and SnO or SnO_2 were prepared and heated in air at 1400°C for two hours. The following compositions were prepared:

95% ZnO + 5% SnO
90% ZnO + 10% SnO
85% ZnO + 15% SnO
67% ZnO + 33% SnO_2

Examination of the X-ray diffraction patterns of these samples showed that a second phase was formed by reaction of the mixtures. Since the new diffraction peaks were similar to those present in the pattern of the 67% ZnO + 33% SnO_2 sample and since some of the peaks characteristic of ZnO disappeared completely in this pattern, it is likely that the phase formed was Zn_2SnO_4. The positions of the peaks in the back-reflection region that were characteristic of ZnO shifted very little so it is likely that very little tin went into solution in the ZnO under these treatment conditions.

ZnO-CuO solid solutions. Solid solutions in the system ZnO-CuO were prepared by heating the oxide mixtures at 1400°C for 2-1/2 hours. The lattice constants were slightly lower than those of pure ZnO indicating that at least some copper went into solution in the zinc oxide. The thermal expansion data for a composition 80% ZnO + 20% CuO are presented in Table XI and Figure 9. The thermal expansion values for both the "a" axis and "c" axis directions are higher than were observed for the pure ZnO. The thermal expansion anisotropy is somewhat reduced but owing to the large amount of CuO available for reaction in

TABLE XI

Thermal Expansion Data
80% ZnO + 20% CuO
Fired at 1400°C for 2-1/2 Hours
Pattern No. 40

Temp. °C	Angle 213	Angle 302	d_{213}	d_{302}	a_o	Δa	% Exp	c_o	Δc	% Exp
Rm. T	116.358	121.648	.90650	.88217	3.2481	-	-	5.2034	-	-
200	116.215	121.469	.90720	.88295	3.2515	.0034	.10	5.2048	.0014	.03
400	115.942	121.153	.90855	.88432	3.2567	.0086	.26	5.2110	.0076	.15
600	115.672	120.812	.90989	.88581	3.2628	.0147	.45	5.2134	.0100	.19
800	115.370	120.476	.91141	.88729	3.2681	.0200	.61	5.2223	.0189	.36
1000	115.058	120.132	.91298	.88882	3.2764	.0283	.86	5.2313	.0279	.53

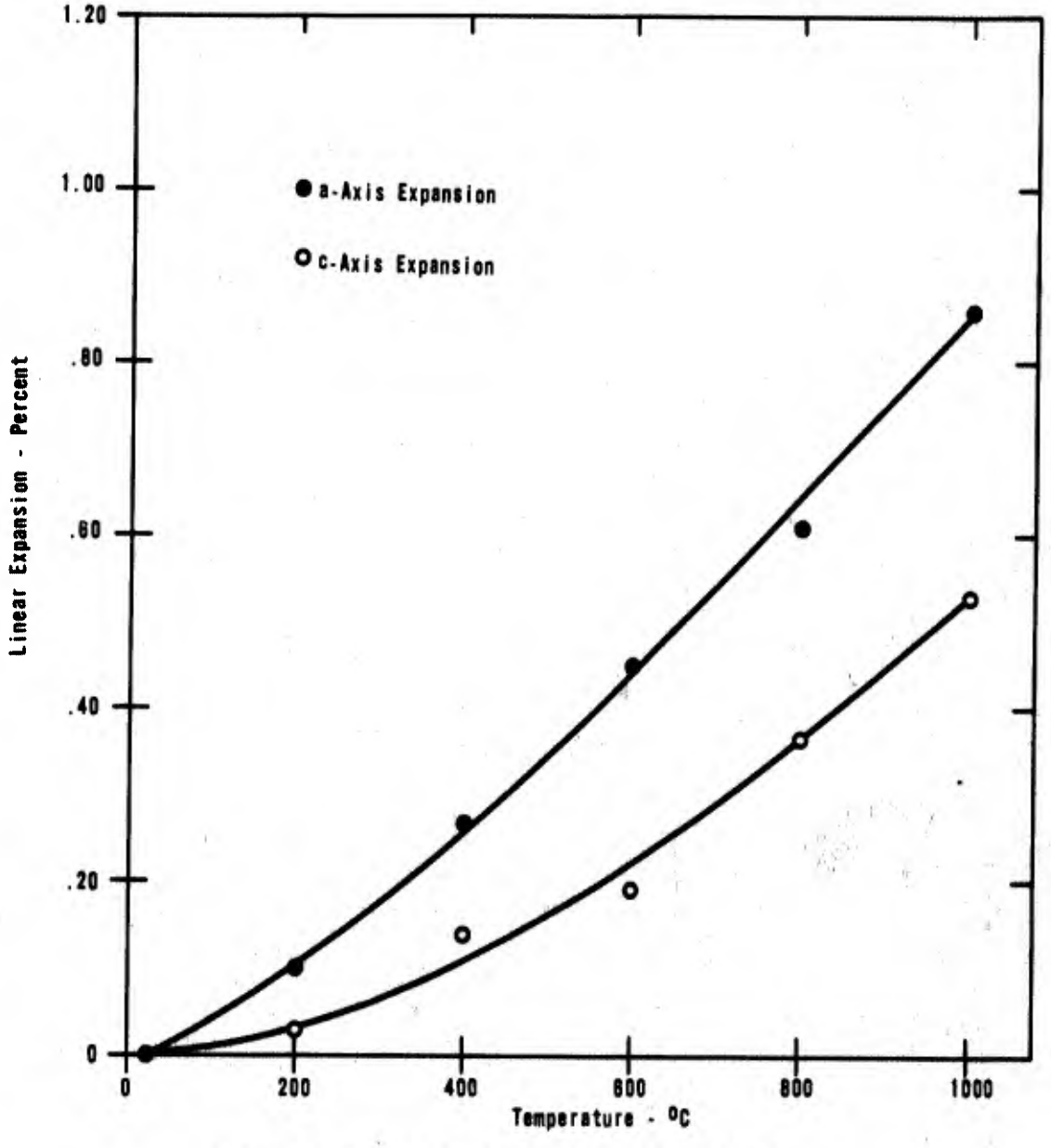

Figure 9 Thermal Expansion of 80% ZnO + 20% CuO
(Pattern No. 40, Miller Indices 213, 302)

this composition it seems unpromising to add more CuO in an attempt to obtain further reduction of the anisotropy.

ZnO-Li_2O solid solutions. A solid solution of lithium in ZnO was prepared by heating the composition 90% ZnO + 10% $1/2Li_2O$ to 1200°C for one hour. Lithium carbonate was used as the source of lithium. The resulting peaks were rather broad so another sample was prepared by firing at 1300°C for five hours. In this case the back-reflection peaks were much sharper. The lattice constants were determined and are only slightly smaller than the lattice constants of pure ZnO. This observation coupled with the fact that the ionic radius of Li^+ (0.68Å) is substantially smaller than that of Zn^{2+} and no evidence of a second phase was available from the X-ray diffraction pattern indicates that some of the lithium may have been lost by evaporation and only a small amount may have gone into solution.

The thermal expansion data are presented in Table XII and Figure 10. The "a" axis and "c" axis expansions are both slightly greater than those of pure ZnO and there is little change in the thermal expansion anisotropy.

ZnO-V_2O_5 solid solutions. The following compositions were prepared:

90% ZnO + 10% $1/2V_2O_5$ at 1200°C for 1 hour
90% ZnO + 10% $1/2V_2O_5$ at 1000°C for 5 hours
80% ZnO + 20% $1/2V_2O_5$ at 1000°C for 5 hours.

The X-ray diffraction patterns of all of the samples showed

TABLE XII

Thermal Expansion Data
90% ZnO + 10% $1/2Li_2O$
1300°C for 5 hours
Pattern No. 12

Temp. °C	Angle 205	Angle 302	d_{205}	d_{302}	a_o	Δa	% Exp	c_o	Δc	% Exp
Rm. T	134.044	121.684	.83663	.88203	3.2477	-	-	5.2043	-	-
200	133.820	121.466	.83733	.88296	3.2513	.0036	.11	5.2079	.0036	.07
400	133.504	121.144	.83832	.88436	3.2567	.0090	.28	5.2127	.0083	.16
600	133.188	120.830	.83932	.88573	3.2620	.0143	.44	5.2176	.0133	.26
800	132.838	120.438	.84043	.88746	3.2688	.0211	.65	5.2224	.0181	.35
1000	132.472	120.088	.84160	.88901	3.2748	.0271	.83	5.2284	.0241	.46

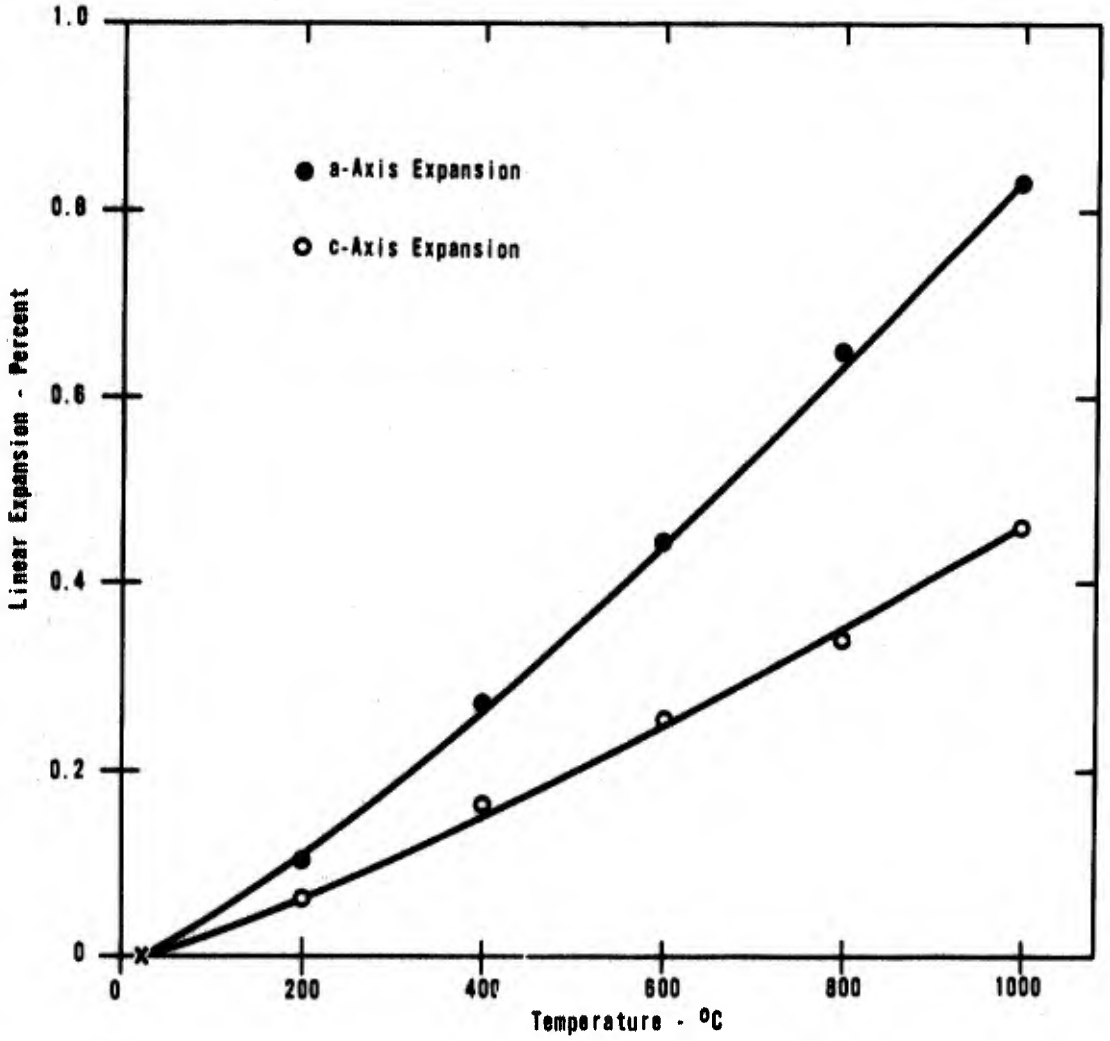

Figure 10 Thermal Expansion of 90% ZnO + 10% 1/2 Li_2O
(Pattern No. 12, Miller Indices 205,302)

evidence of the presence of a second phase and the positions of the peaks in the back-reflection region did not shift as it is probable they would do if substantial solid solution occurred. Therefore, thermal expansion measurements were not performed on these samples.

ZnO-Fe_3O_4 solid solution. The composition 90% ZnO + 10% Fe_3O_4 was prepared by heating the mixed oxides at 1400°C for 2-1/2 hours. An X-ray pattern of the sample showed the presence of a second phase and no back-reflection peaks. No further investigation of these compositions is planned.

ZnO-CdO solid solutions. The composition 90% ZnO + 10% CdO was prepared by heating the mixed oxides at 1400°C for 2-1/2 hours. An X-ray pattern of the sample showed small peaks characteristic of CdO indicating the presence of a small amount of second phase. The back-reflection peaks were rather broad. A relatively large shift in peak positions to lower angles was observed. This shift indicates an increase in unit cell dimensions resulting from solution of the larger Cd^{2+} ions (0.97Å) in ZnO.

Based on the above observations it seems likely that considerable solid solution formation occurred. It is planned to attempt to improve the sharpness of the back-reflection peaks and then measure the thermal expansion properties.

ZnO-MnO_2 solid solutions. The composition 90% ZnO + 10% MnO_2 was prepared by heating the mixed oxides at 1400°C for 2-1/2 hours. The X-ray pattern for the sample did not show evidence of a second phase. The back-reflection peaks were rather broad and were shifted to lower angles indicating larger lattice spacings.

Based on the above observations, it seems likely that considerable solid solution formation occurred. It is planned to attempt to improve the quality of the back-reflection peaks and then measure the thermal expansion properties.

ZnO-MgO solid solutions. The composition 90% ZnO + 10% MgO was prepared by heating the mixed oxides at 1400°C for 2-1/2 hours. An X-ray pattern of the sample showed no evidence of a second phase. This is rather surprizing since the phase diagram shows less than 5% MgO in solution in ZnO.

The back-reflection peaks were broad. The 220 peak was shifted to a lower angle indicating that the a_o value is increased by the presence of the MgO. This increase was not expected because the ionic radius of Mg^{2+} (0.67Å) is less than that of Zn^{2+}. In addition, the 205 peak was shifted to a higher angle indicating a probable decrease in c_o. Based upon the earlier discussion of the relationship of the difference between the actual and expected changes in the lattice constants and the changes in the expansion coefficients, one would predict a marked decrease in the expansion coefficient in the "a" axis direction and a substantial decrease in the expansion anisotropy.

It is planned to prepare other samples at higher temperatures in an attempt to improve the back-reflection peaks and then attempt to measure the expansion coefficients to verify this prediction.

IV. STRENGTHENING OXIDES BY REDUCTION OF THERMAL EXPANSION ANISOTROPY

(A). Introduction

From previous research, several compositions with substantially reduced thermal expansion anisotropy are known. These compositions include the following:

$$90\%\ TiO_2 + 10\%\ VO_2 \quad (7)$$
$$72\%\ Al_2O_3 + 28\%\ Cr_2O_3 \quad (8)$$

The thermal expansion curves for these compositions, compared with the pure oxides are given in Figures 11 and 12. In addition, it is known that additions of VO_2 in solution in SnO_2 can be used to reduce the thermal expansion anisotropy of SnO_2.(7)

In order to establish that a strengthening effect occurs when polycrystalline bodies are prepared from compositions having reduced thermal expansion anisotropy and, thus, smaller localized stresses, it is necessary to compare the strengths of bodies having the same grain size and porosity. It is desirable to investigate the strengths of nearly non-porous bodies with a wide range of grain sizes because of the pronounced dependence of strength on grain size. Furthermore, it is possible that the anisotropy itself is responsible for the grain size dependence of strength over a range of grain sizes. Even though classical mechanics does not predict an increase in local stress with increasing grain size, the tendency toward crack formation may depend on grain size. For example, it is well known that the cracks formed in polycrystalline bodies

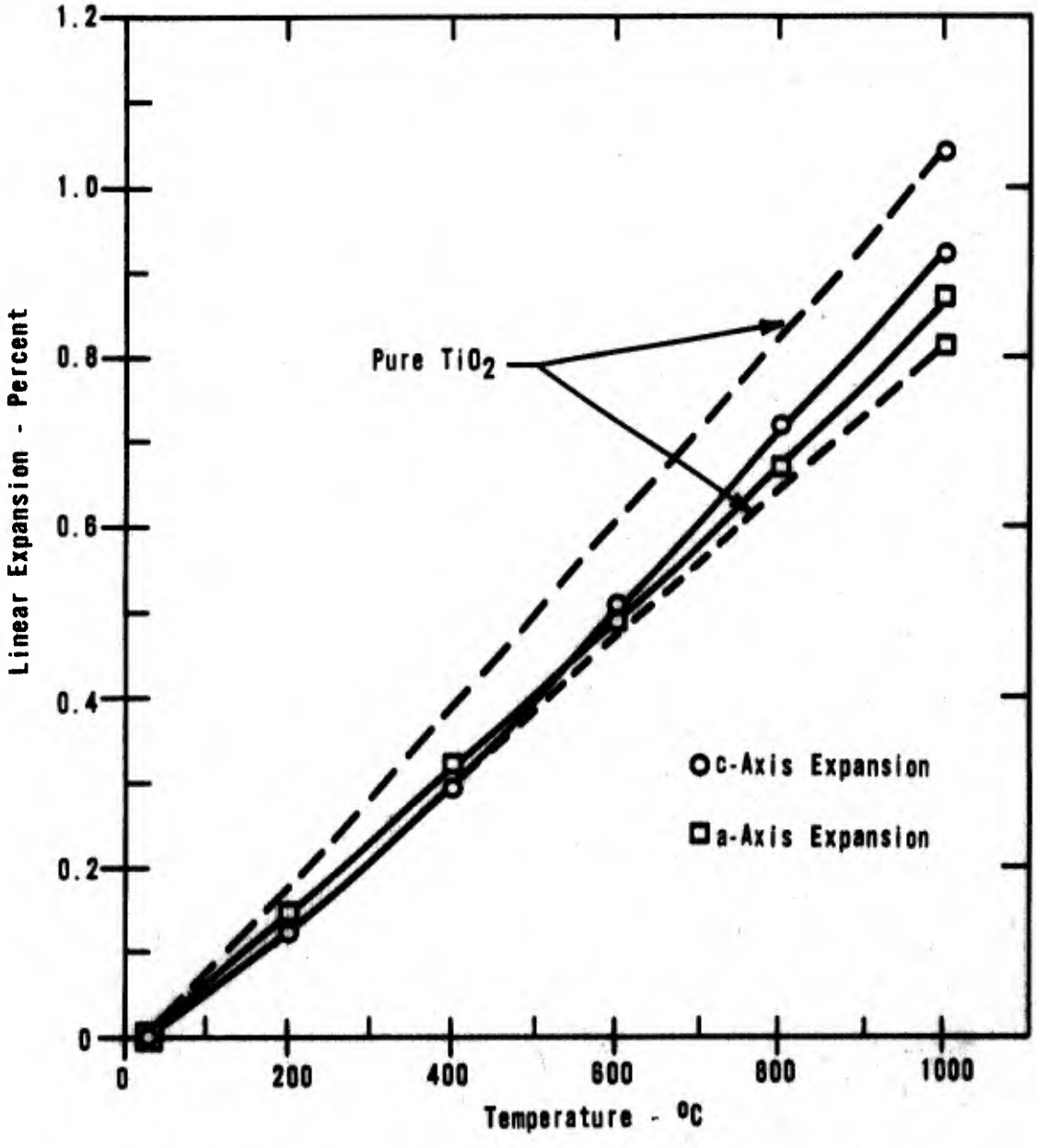

Figure 11 Linear Thermal Expansion of 90% TiO_2 + 10% VO_2

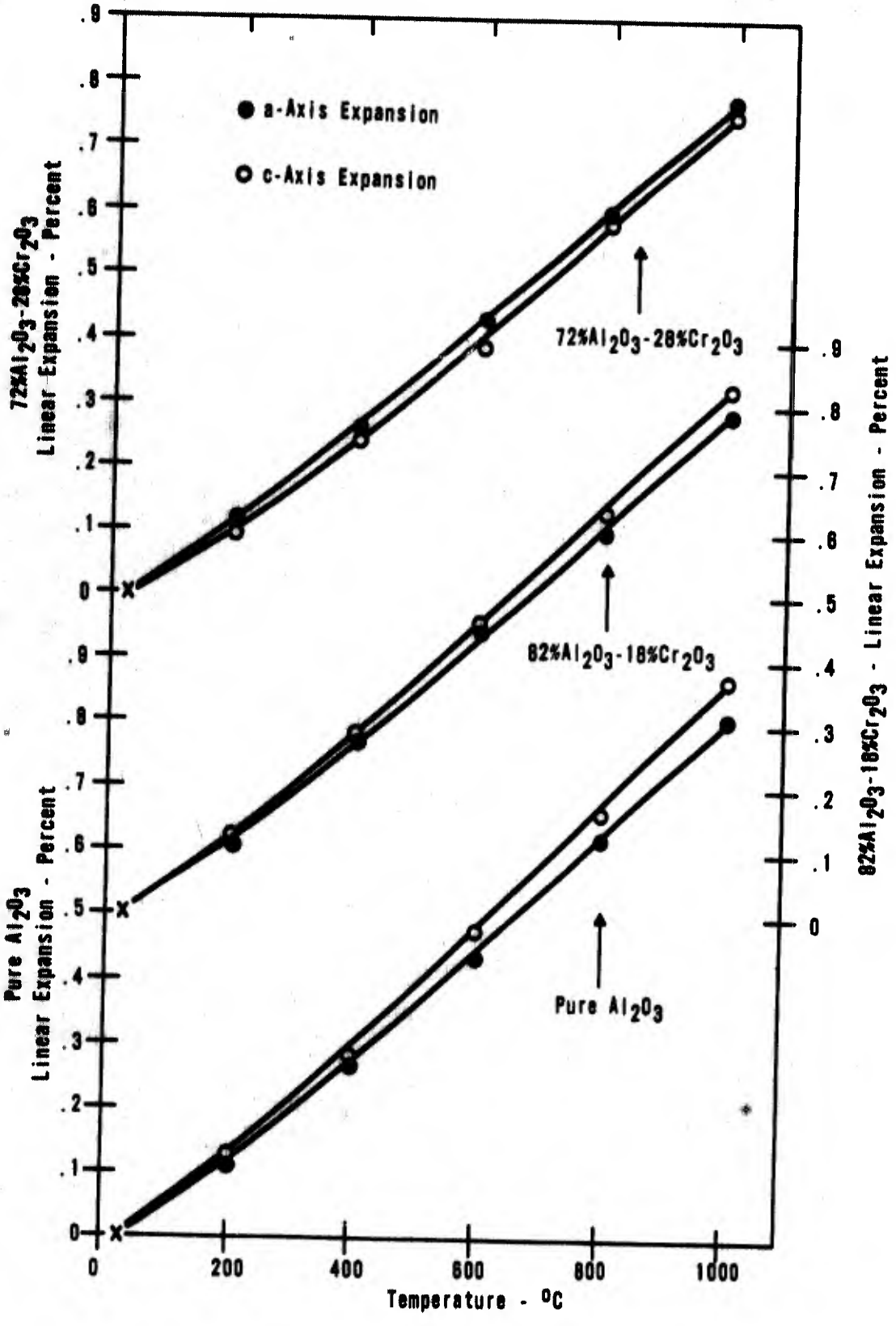

Figure 12 Thermal Expansion of Al_2O_3-Cr_2O_3 Solid Solutions

composed of anisotropic crystals, when these bodies are cooled from sintering temperatures, have a tendency to seize when the temperature is raised again. This seizing process is responsible for some features of the thermal expansion hysteresis observed for these polycrystalline bodies.[4,6] It is evident that there is a range of crack widths in which the crack is not stable. If a crack must open to a particular minimum width by relieving tensile stresses and recovering strain energy stored as a result of expansion anisotropy, it seems likely to occur in large grains rather than in small ones. For example, a simple calculation based on Hookes law and assuming typical strengths shows that a grain size of at least 1 μ is necessary in order to have residual elongations of individual grains of at least 10Å. It is reasonable that the surface forces could act over even larger distances to cause seizing. Presumably, for grain sizes less than one micron, localized crack formation will not occur because, if one did form, seizing would occur and cause it to close again. However, in larger grain size bodies localized cracks may form as a result of the combined effect of residual stresses and applied loads, leading to lower strengths.

It is significant that the degree of thermal expansion anisotropy of crystals in important oxide bodies consisting of corundum (Al_2O_3), rutile (TiO_2) or bromellite (BeO), is great enough so that the residual elongations in the high expansion directions of small crystals cooled in a homogeneous matrix from the sintering temperature to room temperature, are of the order of 10-100Å.

It is also interesting to compare the available strength-grain size information from the point of view of the degree of anisotropy of the individual phases. Of special interest is the fact that MgO which has isotropic thermal expansion properties but has anisotropic elastic constants, has only a small dependence of strength on grain size. The materials that have anisotropic thermal expansion properties have greater dependence of strength on grain size. Available literature information is collected in Table XIII. The increasing dependence of the strength on grain size as the degree of anisotropy increases is evident from the data given. In addition, in rutile bodies of 28 μ grain size, the localized cracks open to a width where they are easily observable by optical microscopy[22] even without superimposing externally applied loads. Rutile (TiO_2) has larger thermal expansion anisotropy ($24 \times 10^{-7}/°C$) than Al_2O_3 or BeO and is presumed to be weak at temperatures below which the cracks form. Increases in strength with increasing temperature are well known for materials like graphite that have very great expansion anisotropy.

The small amount of microscopic evidence available in the literature indicates that the cracks formed as a result of thermal expansion anisotropy are very thin. It is likely that these cracks have high stress concentration factors making them more likely sources of failure than voids formed at high temperatures where diffusion tends to round any sharp cracks.

Based upon this approach, the assumed fracture mechanism for single phase bodies composed of anisotropic crystals is

TABLE XIII

Degrees of Anisotropy and Grain Size Exponents for some Oxides

Material	Elastic Anisotropy	Thermal Expansion Anisotropy $°C^{-1}$ $\Delta\alpha = \alpha_c - \alpha_a$	Grain Size Exponent Note (1)
MgO (periclase)	yes	none	$-1/6$ (4)
Al_2O_3	yes	6.6×10^{-7} (2) (Rm.T-1000°C)	$-1/3$ (4)
BeO	yes	10.4×10^{-7} (3) (27-1000°C)	-1 (5)

Notes

(1) the exponent x in $S = S_o d^x$ in which d is the grain size, S_o is the strength at unit grain size, and S is the strength at grain size d.
(2) data from Merz, Smyth and Kirchner (18)
(3) previously unpublished data, see Figure 13
(4) data from Spriggs and Vasilos (19)
(5) data from Quirk et al (20) as quoted by Carniglia (21)

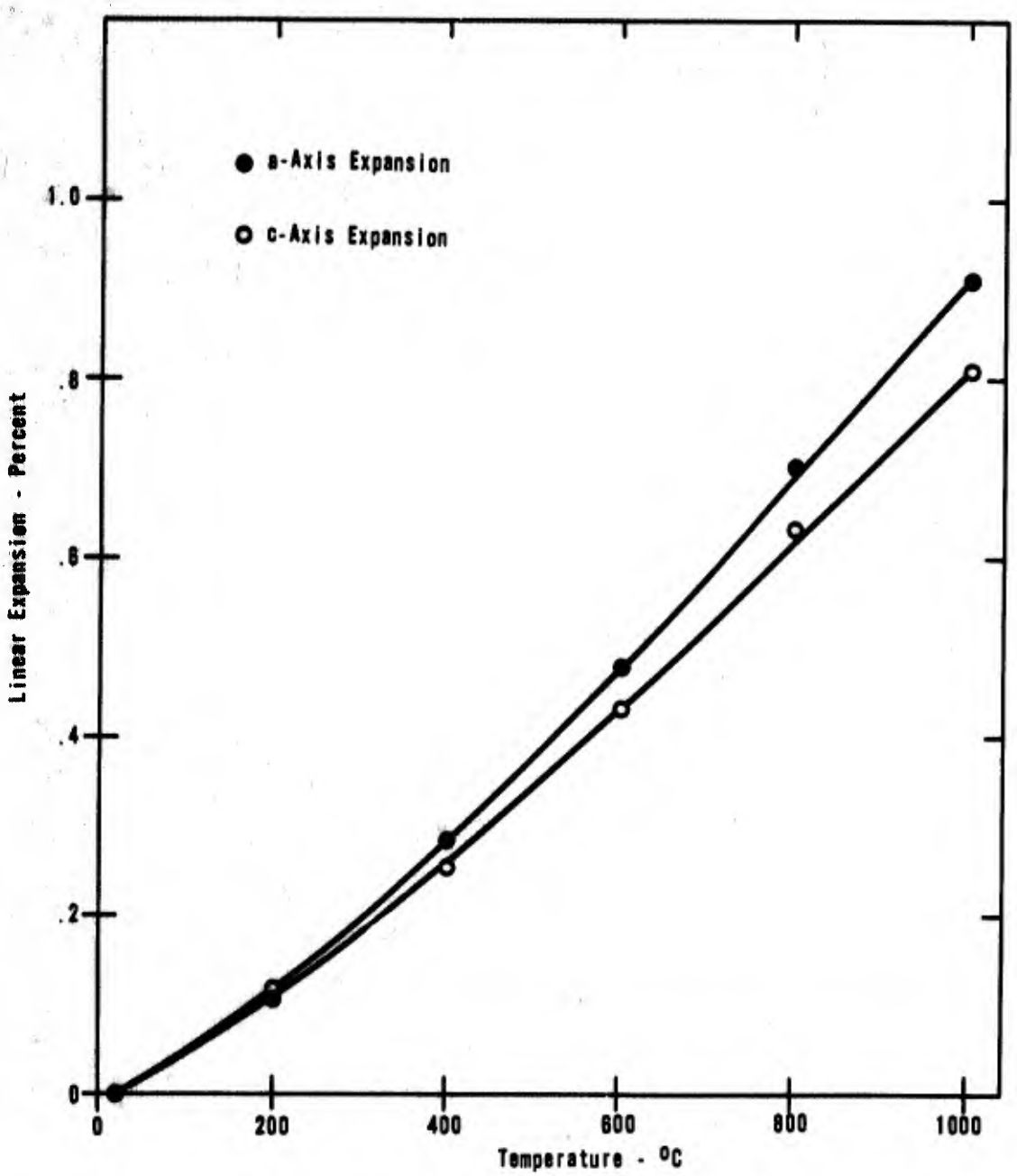

Figure 13 Thermal Expansion of BeO
(Miller Indices 114,300)

as follows:

1. The residual stresses resulting from thermal expansion anisotropy, the localized stresses resulting from elastic anisotropy, and the large scale stresses resulting from applied loads combine to cause regions of high localized stress.

2. Localized fractures will occur at the largest grains present that have the most disadvantageous orientations, when the stress is sufficient to overcome the inherent strength of the particular locality and when the total deformation of the grain is sufficient so that the crack formed will open beyond the width at which seizing would occur. The reason the cracks occur at the largest grains is that only in these grains is there enough total deformation to attain the required crack width to overcome the tendency to seize.

3. The orientation and the sharpness of these cracks will tend to permit propagation of these cracks at lower applied loads than are required to propagate other types of cracks.

The above assumptions lead one to expect the following features to be characteristic of nearly non-porous materials composed of crystals with reduced expansion anisotropy:

1. At small grain sizes the observed strengths should be those inherent in the composition.

2. The grain size dependence of the strength should be smaller than that of the comparable pure oxides.

3. If the composition is inherently as strong or stronger than the pure oxides, the smaller grain size dependence will lead to higher strengths at large grain sizes.

4. Some of the most promising uses of these materials are expected in applications in which the materials are subjected to temperatures great enough to cause grain growth followed by loading at relatively low temperatures.

The experiments used to attempt to show the strengthening effect in compositions with reduced expansion anisotropy were designed to show improved strength and reduction of the grain size dependence of the strength.

(B). Sample Preparation

Discs of the compositions with reduced thermal expansion anisotropy and the comparable pure oxides were prepared by reactive hot pressing in a resistance furnace with 40% Rh - 60% Pt windings. Bars were cut from these discs by diamond sawing. In some cases the bars were reheated to grow the grains. The bars were polished by diamond lapping and the strength was measured in flexure by three-point loading on a one-half inch span. The bulk density, porosity and grain size of the samples were measured.

(C). Results and Discussion

Al_2O_3-Cr_2O_3 solid solutions. These bodies were prepared by reactive hot pressing of coprecipitated hydroxides from a solution having aluminum and chromium present in the molar ratio 72:28. The precipitate was dried at 110°C, prepressed at 5000 psi and then hot pressed in between graphite discs, with an alumina die body and silicon carbide punches. The pure alumina samples were prepared by reactive hot pressing of $Al(OH)_3 \cdot nH_2O$.

The pressing conditions, refiring conditions, bulk density, grain size and flexural strength of the individual samples of the 72% Al_2O_3-28% Cr_2O_5 are presented in Table XIV. The similar data for pure Al_2O_3 are given in Table XV.

The porosities of the samples vary over a wide range. Some of the more porous samples are surprisingly strong. When

TABLE XIV

72% Al_2O_3-28% Cr_2O_3 Samples Prepared by Reactive Hot Pressing of Precipitated Hydroxides (5000 psi)

Sample No.	Pressing Conditions Temp.°C	Time-Hours	Refiring Conditions Temp.°C	Time-Hours	Relative Bulk Density %	Grain Size Range μ	Max. μ	Flexural Strength psi
1	1480	2	-	-	99.0	2-9	11	53,200
2	1480	2	-	-	96.6	5-16	24	46,300
3	1480	2	-	-	98.1	2-15	23	63,700
4	1480	2	-	-	98.9	2-15	23	61,200
5	1480	2	-	-	89.4	1-3	4	55,900
6	1480	2	-	-	82.3	2-5	7	46,600
7	1480	2	1600	2-1/2	96.7	6-19	20	43,900
8	1480	2	1650(3)(5)	4	98.7	4-7	12	43,200
9	1480	2	1650(3)(5)	4	97.7	6-16	40	28,900
10	1480	2	1650(3)(5)	4	97.7	6-16	40	37,700
11	1480	2	1600(4)	6	99.9	5-25	35	64,900
12	1480	2	1600	12	97.5	2-12	16	28,100
13	1480	2	1600(4)	12	97.0	5-32	48	43,600
14	1480(1)	2	-	-	97.0	5-10	16	55,600
15	1480(2)	2	-	-	83.0	4-8	30	31,300

Notes
(1) Precipitate calcined before pressing 1600°C, 6 hours
(2) 5% of mat'l precalcined at 1650°C for 2 hours
(3) Packed in 72% Al_2O_3-28% Cr_2O_3 powder to prevent vaporization of Cr_2O_3
(4) Packed in Cr_2O_3 powder to prevent vaporization of Cr_2O_3
(5) May be intergranular fracture

TABLE XV

Alumina Samples Prepared by Reactive Hot Pressing of $Al(OH)_3 \cdot nH_2O$ (5,000 psi)

Sample No.	Pressing Conditions Temp.°C	Time-Hours	Refiring Conditions Temp.°C	Time-Hours	Relative Bulk Density %	Grain Size Range μ	Grain Size Max. μ	Flexural Strength psi
1	1480	2	-	-	97.2	2-5	8	62,400
2	1480	2	-	-	98.1	1-3	5	64,200
3	1480	2	1600	2	97.4	2-6	9	61,700
4	1480	2	1600	2	89.5	3-5	10	44,700
5	1480	2	1600	2-1/2	96.8	5-16	24	86,000*
6	1480	2	1600	2-1/2	87.5	4-15	20	53,100
7	1480	2	1600	4	92.0	2-7	10	63,600
8	1480	2	1600	10-1/2	90.0	20-60	100	29,600
9	1400	2	1600	12	96.5	25-90	150	28,500

* Sample hot worked by squeezing out of die.

these data were corrected to zero porosity using the method described by Spriggs,[19] the resulting strength values were unreasonably high. These high values result from non-uniform distribution of porosity in the samples. Since three-point loading was used, only the center of the disc was tested for strength, whereas the test bars contained considerable material from the edges. Therefore, further analysis of the data was restricted to samples having porosities of less than 3.5 volume percent.

The grain sizes of the pure alumina samples were quite small in the "as pressed" condition. The grain size increased substantially as a result of refiring at 1600°C. In the "as pressed" condition the grain size of the 72% Al_2O_3-28% Cr_2O_3 samples was greater than the pure Al_2O_3. In addition, the grains show little tendency to grow during subsequent heat treatment. Therefore, the available grain sizes for the solid solution samples fall in the middle of the range represented in the alumina samples.

The few suitable data points for the pure alumina were used to construct a curve of the grain size dependence of the strength in a manner similar to that used by Spriggs and Vasilos.[19] The dotted line in Figure 14 represents these data based upon maximum grain size and strength values not corrected to zero porosity. Similar data based upon average grain size and strengths corrected to zero porosity are given in Figure 15. In each case the lines fall above the curve presented by Spriggs and Vasilos perhaps because of the small sample size and the

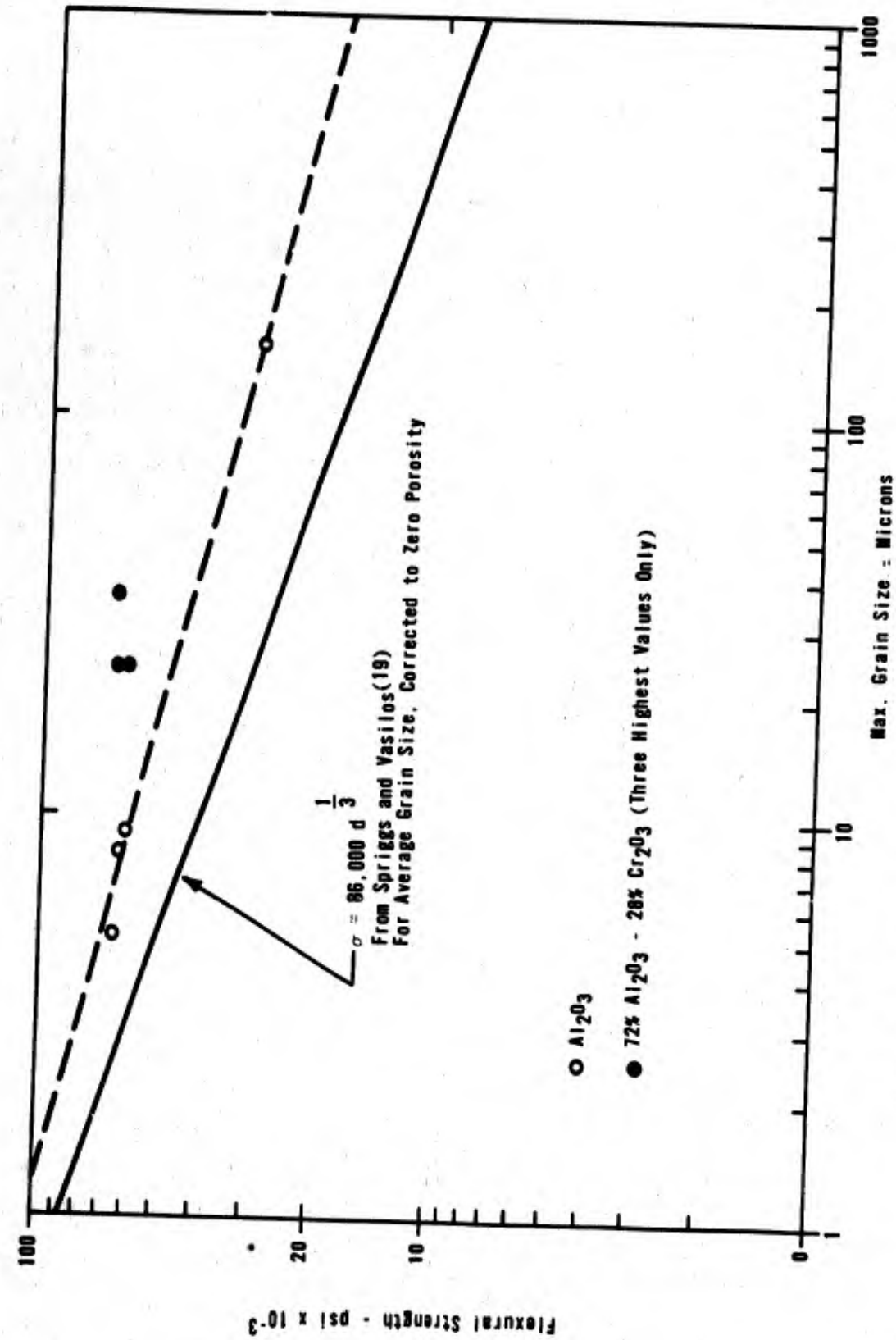

Figure 14 Strength Vs. Max. Grain Size, Data Not Corrected to Zero Porosity

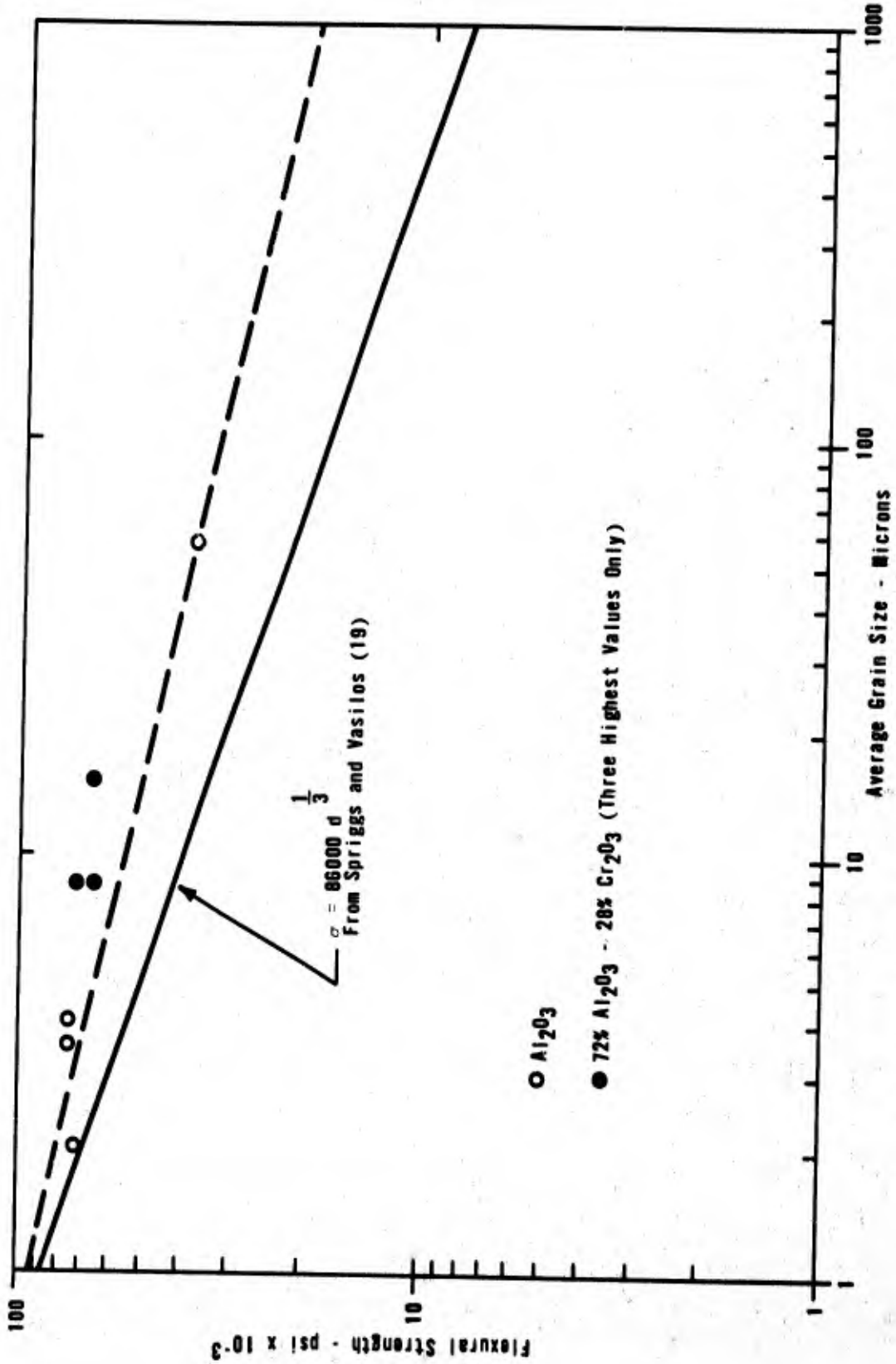

Figure 15 Strength Vs Average Grain Size, Data Corrected to Zero Porosity

three-point loading compared with four-point loading on a 1.5 in. span in the referenced experiments. The slopes determined by the present data are slightly lower than those determined by the referenced data.

The data for the three strongest solid solution samples are plotted in the figures. These strength values constitute preliminary evidence that stronger bodies can be prepared using compositions with reduced thermal expansion anisotropy.

TiO_2-VO_2 solid solutions. Samples with the composition 90% TiO_2-10% VO_2 were prepared by hot pressing the mixed oxides. The materials used were TAM Heavy Grade TiO_2 and Fisher reagent grade V_2O_5. Samples of "pure" TiO_2 were prepared from the Heavy Grade TiO_2.

The "pure" material pressed to 98.9% relative bulk density with a grain size of about one micron in one hour at 1150°C. The flexural strength was 38,700 psi. However, the 90% TiO_2-10% VO_2 mixtures reacted with the die materials in every case and no satisfactory samples were prepared.

V. CONCLUSIONS

1. In pure oxides or solid solutions lattice constants that are larger than expected, based upon the ion sizes, are associated with the lower values of expansion coefficient in the same crystallographic direction and lattice constants that are smaller than expected are associated with higher values of expansion coefficient. Using this approach to predicting the changes in thermal expansion coefficients as various solid solution forming materials are added to an oxide lattice, it is hoped that faster progress can be achieved toward reduction of thermal expansion anisotropy.

2. A solid solution having the nominal composition 60% TiO_2-20% $1/2Ga_2O_3$-20% VO_2 has substantially lower thermal expansion anisotropy than pure TiO_2.

3. Formation of microcracks as a result of localized stresses arising from thermal expansion and elastic anisotropy may occur only in relatively large grains because of the existence of a range of crack widths below some maximum size in which a crack is not stable because of a tendency to seize. Therefore, the grain size dependence of strength may depend upon the degree of thermal expansion and elastic anisotropy. If this is true, it should be possible to demonstrate a smaller grain size dependence of strength for compositions with reduced thermal expansion anisctropy.

4. Preliminary evidence of improved strength in an intermediate grain size range for the composition 72% Al_2O_3-28% Cr_2O_3 which has reduced thermal expansion anisotropy was presented.

VI. REFERENCES

1. H.P. Kirchner and R.M. Gruver, "Chemical Strengthening of Polycrystalline Ceramics," J. Am. Ceram. Soc. 49(6) 330-333 (June, 1966).

2. H.P. Kirchner, R.M. Gruver and R.E. Walker, "Chemically Strengthened, Leached Alumina and Spinel," J. Am. Ceram. Soc. 50(4) 169-173 (April, 1967).

3. H.P. Kirchner, R.M. Gruver and R.E. Walker, "Chemical Strengthening of Polycrystalline Alumina," Paper No. 9-J2-67, Annual Meeting of the American Ceramic Society (May, 1967).

4. W.R. Buessem, N.R. Thielke and R.V. Sarakauskas, "Thermal Expansion Hystiresis of Aluminum Titanate," Ceram. Age 60 (5) 38-40 (1952).

5. F.J.P. Clarke, "Residual Strain and the Fracture Stress-Grain Size Relationship in Brittle Solids," Acta Metallurgica 12, 139-143 (February, 1964).

6. W.R. Buessem and F.F. Lange, "Residual Stresses in Anisotropic Ceramics," Interceram 15(3) 229-231 (1966).

7. K.M. Merz, W.R. Brown, and H.P. Kirchner, Thermal Expansion Anisotropy of Oxide Solid Solutions," J. Am. Ceram. Soc. 45(11) 531-536 (November, 1962).

8. H.P. Kirchner, R.M. Gruver, and R.E. Walker, "Chemical Strengthening of Ceramic Materials," Linden Laboratories, Inc. Summary Report Contract No. NOw 65-0407-c (May, 1966).

9. J.C. Stradley, T.S. Shevlin and J.O. Everhart, "Stresses in Polycomponent Solid Ceramics or Cermets," Ohio State University Res. Found. Prog. Report 806-1, Contract No. AF 35(616)-5515 (July, 1958).

10. P. Wen, J.J. Brown and F.A. Hummel, "Dilatometer and X-ray Data for Zinc Compounds I," Trans. Brit. Ceram. Soc. 63(9) 501-508 (September, 1964).

11. J.J. Brown and F.A. Hummel, "Dilatometric and X-ray Data for Zinc Compounds II. Phosphates and Vanadates," Trans. Brit. Ceram. Soc. 64(8) 387-396 (August, 1965).

12. W.J. Rae, H.A. Scheetz and H.P. Kirchner, "A Study of Meteorite Impact Phenomena," Cornell Aeronautical Laboratory Report No. RM-1655-M-2 (June, 1962).

13. J.F. Sarver, "Thermal Expansion Data for Rutile-Type GeO_2," J. Am. Ceram. Soc. 46(4) 195-196 (April, 1963).

14. D.P. Riley, "Thermal Expansion of Graphite: Part II," Theoretical Proc. Phys. Soc. (London) 57, 486-495 (1945).

15. E.M. Levin, C.R. Robins and H.F. McMurdie, "Phase Diagrams for Ceramists," American Ceramic Society, Columbus (1964).

16. H.E. Swanson and R.K. Fuyat, "Standard X-ray Diffraction Powder Patterns," National Bureau of Standards Circular 539 Volume II (June, 1953).

17. R.J. Beals and R.L. Cook, "Directional Dilatation of Crystal Lattices at Elevated Temperatures," J. Am. Ceram. Soc. 40(8) 279-284 (August, 1957).

18. K.M. Merz, H.T. Smyth and H.P. Kirchner, "The Thermal Expansion of Ceramic Materials," Cornell Aeronautical Laboratory Report PI-1273-M-8, Contract No. NOrd-18419 (September, 1960).

19. R.M. Spriggs and T. Vasilos, "Effect of Grain Size on Transverse Bend Strength of Alumina and Magnesia," J. Am. Ceram. Soc. 46(5) 224-228 (May, 1963).

20. J.F. Quirk, N.B. Mosely and W.H. Duckworth, "Characterization of Sinterable Oxide Powders: I, BeO," J. Am. Ceram. Soc. 40(12) 416-419 (December, 1957).

21. S.C. Carniglia, "Petch Relation in Single-Phase Oxide Ceramics," J. Am. Ceram. Soc. 48(11) 580-583 (November, 1965).

22. F.R. Charvat and W.D. Kingery, "Thermal Conductivity: XIII, Effect of Microstructure on Conductivity of Single-Phase Ceramics," J. Am. Ceram. Soc. 40(9) 306-315 (September, 1957).

DISTRIBUTION LIST

Chief of Naval Research (3)
Department of the Navy
Attn: Code 423
Washington, D.C. 20360

Director (1)
Office of Naval Research
Branch Office
495 Summer Street
Boston, Mass. 02210

Commanding Officer (1)
Office of Naval Research
New York Area Office
207 West 24th Street
New York, N.Y. 10011

Director (1)
Office of Naval Research
Branch Office
219 South Dearborn Street
Chicago, Ill. 60604

Director (1)
Office of Naval Research
Branch Office
1030 East Green Street
Pasadena, California 91101

Comanding Officer (1)
Office of Naval Research
San Francisco Area Office
1076 Mission Street
San Francisco, Calif. 94103

Assistant Attache for Research (5)
Office of Naval Research
Branch Office, London
FPO New York 09510

Commander (1)
Naval Ship Systems Command, Hqts.
Department of the Navy
Attn: Code 0342
Washington, D.C. 20360

Commander (1)
Department of the Navy
Naval Ship Engineering Center
Attn: Code 6101
Washington, D.C. 20360

Director
U.S. Naval Research Laboratory
Washington, D.C. 20390
Attn: Technical Information
Officer, Code 2000 (4)
Code 2020 (1)
Code 6200 (1)
Code 6300 (2)
Code 6100 (1)

Commander
Naval Air Systems Command, Hqts.
Department of the Navy
Washington, D.C. 20360
Attn: Code AIR 320A (1)
Code AIR 5203 (1)

Commander (1)
Naval Ordnance Systems Command, Hqts.
Department of the Navy
Attn: Code ORD 033
Washington, D.C. 20360

Commanding Officer (1)
Naval Air Development Center
Aeronautical Materials Div.
Attn: Code MAM
Johnsville
Warminster, Pa. 18974

Commanding Officer (1)
U.S. Naval Ordnance Laboratory
White Oak, Md. 20910
Attn: Code 210

Commanding Officer (1)
U.S. Naval Weapons Laboratory
Dahlgren, Virginia 22448
Attn: Research Division

National Bureau of Standards
Washington, D.C. 20234
Attn: Metallurgy Division (1)
Inorganic Materials Div. (1)

Commanding Officer (1)
Army Research Office, Durham
Attn: Metallurgy & Ceramics Div.
Box CM, Duke Station
Durham, North Carolina 27706

Naval Ships R&D Center (1)
Annapolis Division
Annapolis, Maryland 21402

Naval Applied Science Lab. (1)
Naval Base
Attn: Code 735
Brooklyn, New York 11251

Commanding Officer (1)
Naval Ships R&D Center
Attn: Code 735
Washington, D.C. 20007

U.S. Naval Postgraduate School
Monterey, California 93940
Attn: Dept. of Chemistry and (1)
Material Science

Commander (1)
Naval Weapons Center
Attn: Code 5560
China Lake, California 93555

Commander (1)
Naval Undersea Warfare Center
3202 E. Foothill Boulevard
Pasadena, California 91107

Defense Documentation Center (20)
Cameron Station
Alexandria, Virginia 22314

Commanding Officer
Army Materials & Mechanics
Research Center
Watertown, Mass. 02172
Attn:
Res. Programs Office(AMXMR-P) (1)
Technical Library(AMXMR-ATL) (1)

University of California (1)
Radiation Laboratory
Information Division
Room 128, Building 50
Berkeley, California 94720

Commanding Officer (1)
U.S. Naval Ordnance Underwater
Station
Newport, Rhode Island 02840

U.S. Air Force (1)
Office of Scientific Research
Attn: Solid State Div. (SRPS)
Washington, D.C. 20333

U.S. Atomic Energy Commission
Washington, D.C. 20545
Attn: Technical Library (1)
Metals & Materials Branch (1)

Argonne National Laboratory (1)
Metallurgy Division
P.O. Box 299
Lemont, Illinois 60439

Brookhaven National Laboratory (1)
Technical Information Division
Attn: Research Library
Upton, Long Island, N.Y. 11973

Union Carbide Nuclear Co.
Oak Ridge National Laboratory
P.O. Box P
Oak Ridge, Tennessee 37830
Attn: Metallurgy Division (1)
Solid State Physics Div. (1)

Los Alamos Scientific Laboratory (1)
Attn: Report Librarian
P.O. Box 1663
Los Alamos, New Mexico 87544

Atomic Energy Commission (1)
New York Operations Office
Attn: Document Custodian
70 Columbus Avenue
New York, N.Y. 10023

NASA Headquarters (1)
Attn: Mr. George C. Deutsch(RRM)
Washington, D.C. 20546

National Academy of Science (1)
Attn: Dr. F.J. Weyl
2101 Constitution Avenue
Washington, D.C. 20418

Air Force Materials Lab (MAMC) (1)
Wright Patterson AFB
Dayton, Ohio 45433

Deep Submergence Systems Project
Attn: DSSP-00111 (1)
Washington, D.C. 20360

Aerospace Research Laboratories (1)
Building 450
Wright Patterson AFB
Dayton, Ohio 45433

Defense Metals Information Center (1)
Battelle Memorial Institute
505 King Avenue
Columbus, Ohio 43201

Evans Signal Laboratory (1)
Army Electronics Command
Solid State Devices Branch
c/o Senior Navy Liaison Officer
Fort Monmouth, New Jersey 07703

Commanding General (1)
U.S. Army, Frankford Arsenal
Attn: Mr. Harold Markus
ORDBA-1320, 64-4
Philadelphia, Pa. 19137

Executive Director (1)
Materials Advisory Board
NAS-NRC
2101 Constitution Avenue
Washington, D.C. 20418

Professor R. Roy (1)
Pennsylvania State University
Materials Research Laboratory
University Park, Pa. 16802

Professor D.H. Whitmore (1)
Northwestern University
Department of Metallurgy
Evanston, Illinois 60201

Professor P.J. Bray (1)
Brown University
Department of Physics
Providence, Rhode Island 02912

Professor W.R. Buessem (1)
Pennsylvania State University
Department of Ceramic Technology
University Park, Pa. 16802

Professor W.D. Kingery (1)
Massachusetts Institute of Technology
Department of Metallurgy
Cambridge, Mass. 02100

Advanced Research Projects Agency (1)
Attn: Dr. R.M. Thomson
Materials Sciences
Washington, D.C. 20301

Army Research Office (1)
Attn: Dr. J. Majowicz
3045 Columbia Pike
Arlington, Virginia 22204

Department of Interior (1)
Bureau of Mines
Attn: Science & Engineering
Advisor
Washington, D.C. 20240

Professor D. Turnbull (1)
Harvard University
Division of Engineering &
Applied Science
Pierce Hall
Cambridge, Mass. 02100

Dr. J.B. Wachtman, Jr. (1)
National Bureau of Standards
Division 9.6
Washington, D.C. 20234

Dr. T. Vasilos (1)
AVCO Corporation
Research & Advanced Development
Division
201 Lowell Street
Wilmington, Mass. 01887

Professor J.D. Mackenzie (1)
Rensselaer Polytechnic Institute
Department of Materials
Engineering
Troy, New York 12181

Dr. S. Blum (1)
Assistant Director, Metals &
Ceramics
Illinois Institute of Technology
10 West 35th Street
Chicago, Illinois 60616

Dr. J.J. Duga (1)
Battelle Memorial Institute
Physics Department
505 King Avenue
Columbus, Ohio 43201

Professor I.B. Cutler (1)
University of Utah
Salt Lake City, Utah 84112

Dr. H.C. Gatos (1)
Massachusetts Institute of Technology
Metallurgy & Electrical Engineering
Cambridge, Mass. 02100

Professor L.H. Van Vlack (1)
University of Michigan
Chemical & Metallurgical Engineering
Ann Arbor, Michigan 48103

Professor J.A. Pask (1)
University of California
Department of Mineral Technology
Berkeley, California 94720

Dr. H.A. Perry (1)
Naval Ordnance Laboratory
Code 230
Silver Spring, Maryland 20910

Dr. Paul Smith (1)
Naval Research Laboratory
Crystals Branch, Code 6430
Washington, D.C. 20390

Dr. James H. Schulman (1)
Naval Research Laboratory
Optical Physics Division
Code 7300
Washington, D.C. 20390

Professor Norbert Kreidl (1)
University of Missouri
Department of Ceramic Engineering
Rolla, Missouri 65401

Dr. J.C. Grosskreutz (1)
Midwest Research Institute
425 Volker Boulevard
Kansas City, Missouri 64110

Professor G.S. Ansell (1)
Rensselaer Polytechnic Institute
Troy, New York 12181

Dr. A.R.C. Westwood (1)
RIAS Division
Martin Marietta Corporation
1450 South Rolling Road
Baltimore, Maryland 21227

Dr. Cyrus Klingsberg (1)
National Academy of Sciences
Division of Engineering
2101 Constitution Avenue, N.W.
Washington, D.C. 20418

Mr. Karl Schwartzwalder (1)
General Motors Corporation
AC Spark Plug Division
Engineering Building
1300 North Dort Highway
Flint, Michigan 48556

Mr. Jesse D. Walton, Jr. (1)
Head, High Temperature Materials Branch
Georgia Institute of Technology
Engineering Experiment Station
Atlanta, Georgia 30332

Dr. R.J. Charles (1)
General Electric Corporation
Metallurgy and Ceramics Laboratory
Schenectady, New York 12301

Professor E.I. Salkovitz (1)
University of Pittsburgh
Metallurgy Department
Pittsburgh, Pa. 15213

Dr. G.M. Muchow (1)
Owens-Illinois Technical Center
1700 North Westwood
Toledo, Ohio 43607

Dr. Philip L. Farnsworth (1)
Battelle Northwest
Materials Department
P.O. Box 999
Richland, Washington 99352

Professor G.R. Miller (1)
University of Utah
Dept. of Ceramic Engineering
Salt Lake City, Utah 84112

Dr. George J. Bair (1)
Director, Technical Staff Services
Corning Glass Works
Corning, New York 14830

Dr. Stephen C. Carniglia (1)
Atomics International Division
North American Aviation, Inc.
P.O. Box 309
Canoga Park, California 91304

U.S. Department of Interior (1)
Bureau of Mines
College Park Metallurgy Research Center
College Park, Maryland 20740

U.S. Department of Interior (1)
Bureau of Mines
Albany Metallurgy Research Center
Albany, Oregon 97321

Dr. S.D. Brown (1)
Principal Scientist
Ceramics Research
Rocketdyne
Canoga Park, California 91304

Dr. David L. Douglass (1)
Stanford Research Institute
Physical Sciences Division
Menlo Park, California 94025

Mr. Laurence E. Ferreira (1)
Coors Porcelain Company
Golden, Colorado 80401

Professor Robert A. Huggins (1)
Stanford University
Department of Materials Science
Stanford, California 94305

Professor Thomas D. McGee (1)
Iowa State University
Ames, Iowa 50010

Office of Naval Research (1)
Physics Branch, Code 421
Washington, D.C. 20360

Professor J.B. Wagner, Jr. (1)
Northwestern University
Dept. of Materials Science
Evanston, Illinois 60201

Commanding Officer (1)
Army Materials & Mechanics Research Center
Watertown, Mass. 02171
Attn: Mr. I. Berman

Commanding General (1)
U.S. Army, Frankford Arsenal
Philadelphia, Pa. 19137
Attn: Dr. Sidney Ross

Battelle Memorial Institute (1)
Defense Ceramic Information Center
505 King Avenue
Columbus, Ohio 43201

BLANK PAGE

Security Classification

DOCUMENT CONTROL DATA - R&D

(Security classification of title, body of abstract and indexing annotation must be entered when the overall report is classified)

1. ORIGINATING ACTIVITY *(Corporate author)*
Linden Laboratories, Inc.

2a. REPORT SECURITY CLASSIFICATION
Unclassified

2b. GROUP

3. REPORT TITLE
Strengthening Oxides by Reduction of Crystal Anisotropy

4. DESCRIPTIVE NOTES *(Type of report and inclusive dates)*
Technical Report No. 1

5. AUTHOR(S) *(Last name, first name, initial)*
Kirchner, Henry P.
Gruver, Robert M.

6. REPORT DATE
August, 1967

7a. TOTAL NO. OF PAGES
65

7b. NO. OF REFS
22

8a. CONTRACT OR GRANT NO.
N00014-66-C0190

b. PROJECT NO.

c. Requisition Number: NR 032-498

d.

9a. ORIGINATOR'S REPORT NUMBER(S)

9b. OTHER REPORT NO(S) *(Any other numbers that may be assigned this report)*

10. AVAILABILITY/LIMITATION NOTICES
Distribution of this report is unlimited

11. SUPPLEMENTARY NOTES

12. SPONSORING MILITARY ACTIVITY
Office of Naval Research
Department of the Navy

13. ABSTRACT

An investigation of the effect of crystal anisotropy on the strength of oxides is described. Solid solutions of various materials in rutile (TiO_2) and zincite (ZnO) were prepared and the thermal expansion properties were measured in an attempt to find compositions with reduced anisotropy.

Bodies composed of 72% Al_2O_3-28% Cr_2O_3 were prepared by reactive hot pressing. Preliminary evidence of a strengthening effect compared with pure Al_2O_3 is presented.

DD FORM 1 JAN 64 1473

Security Classification

14. KEY WORDS	LINK A		LINK B		LINK C	
	ROLE	WT	ROLE	WT	ROLE	WT
thermal expansion elastic properties anisotropy flexural strength localized stresses X-ray diffraction reactive hot pressing solid solution alumina magnesia beryllia titania zinc oxide						

INSTRUCTIONS

1. **ORIGINATING ACTIVITY:** Enter the name and address of the contractor, subcontractor, grantee, Department of Defense activity or other organization *(corporate author)* issuing the report.

2a. **REPORT SECURITY CLASSIFICATION:** Enter the overall security classification of the report. Indicate whether "Restricted Data" is included. Marking is to be in accordance with appropriate security regulations.

2b. **GROUP:** Automatic downgrading is specified in DoD Directive 5200.10 and Armed Forces Industrial Manual. Enter the group number. Also, when applicable, show that optional markings have been used for Group 3 and Group 4 as authorized.

3. **REPORT TITLE:** Enter the complete report title in all capital letters. Titles in all cases should be unclassified. If a meaningful title cannot be selected without classification, show title classification in all capitals in parenthesis immediately following the title.

4. **DESCRIPTIVE NOTES:** If appropriate, enter the type of report, e.g., interim, progress, summary, annual, or final. Give the inclusive dates when a specific reporting period is covered.

5. **AUTHOR(S):** Enter the name(s) of author(s) as shown on or in the report. Enter last name, first name, middle initial. If military, show rank and branch of service. The name of the principal author is an absolute minimum requirement.

6. **REPORT DATE:** Enter the date of the report as day, month, year; or month, year. If more than one date appears on the report, use date of publication.

7a. **TOTAL NUMBER OF PAGES:** The total page count should follow normal pagination procedures, i.e., enter the number of pages containing information.

7b. **NUMBER OF REFERENCES:** Enter the total number of references cited in the report.

8a. **CONTRACT OR GRANT NUMBER:** If appropriate, enter the applicable number of the contract or grant under which the report was written.

8b, 8c, & 8d. **PROJECT NUMBER:** Enter the appropriate military department identification, such as project number, subproject number, system numbers, task number, etc.

9a. **ORIGINATOR'S REPORT NUMBER(S):** Enter the official report number by which the document will be identified and controlled by the originating activity. This number must be unique to this report.

9b. **OTHER REPORT NUMBER(S):** If the report has been assigned any other report numbers *(either by the originator or by the sponsor)*, also enter this number(s).

10. **AVAILABILITY/LIMITATION NOTICES:** Enter any limitations on further dissemination of the report, other than those imposed by security classification, using standard statements such as:

(1) "Qualified requesters may obtain copies of this report from DDC."

(2) "Foreign announcement and dissemination of this report by DDC is not authorized."

(3) "U. S. Government agencies may obtain copies of this report directly from DDC. Other qualified DDC users shall request through

_____."

(4) "U. S. military agencies may obtain copies of this report directly from DDC. Other qualified users shall request through

_____."

(5) "All distribution of this report is controlled. Qualified DDC users shall request through

_____."

If the report has been furnished to the Office of Technical Services, Department of Commerce, for sale to the public, indicate this fact and enter the price, if known.

11. **SUPPLEMENTARY NOTES:** Use for additional explanatory notes.

12. **SPONSORING MILITARY ACTIVITY:** Enter the name of the departmental project office or laboratory sponsoring *(paying for)* the research and development. Include address.

13. **ABSTRACT:** Enter an abstract giving a brief and factual summary of the document indicative of the report, even though it may also appear elsewhere in the body of the technical report. If additional space is required, a continuation sheet shall be attached.

It is highly desirable that the abstract of classified reports be unclassified. Each paragraph of the abstract shall end with an indication of the military security classification of the information in the paragraph, represented as *(TS), (S), (C), or (U)*.

There is no limitation on the length of the abstract. However, the suggested length is from 150 to 225 words.

14. **KEY WORDS:** Key words are technically meaningful terms or short phrases that characterize a report and may be used as index entries for cataloging the report. Key words must be selected so that no security classification is required. Identifiers, such as equipment model designation, trade name, military project code name, geographic location, may be used as key words but will be followed by an indication of technical context. The assignment of links, rules, and weights is optional.